Chemical Science

ROYAL SOCIETY OF CHEMISTRY

EDGE ARTICLE

View Article Online
View Journal

Cite this: DOI: 10.1039/d5sc01502b

All publication charges for this article have been paid for by the Royal Society of Chemistry

Unique selectivity of rare-earth metal ambiphilic carbenes towards organic molecules and novel reactivity patterns with isonitriles†

Fuxiang Chai,[a] Weikang Wu,[a] Thayalan Rajeshkumar,[d] Zeming Huang,[b] Qingbing Yuan,[a] Yun Wei,[a] Laurent Maron *[d] and Shaowu Wang *[bc]

Received 25th February 2025
Accepted 20th May 2025

DOI: 10.1039/d5sc01502b

rsc.li/chemical-science

Studies on the chemistry of highly active rare-earth (RE) metal ambiphilic carbenes face challenges due to the lack of appropriate model molecular platforms because the corresponding ambiphilic carbenes have empty p-orbitals. Here, the synthesis of novel multi-chelated amidate rare-earth metal pincer complexes bearing ambiphilic carbenes is realized by using indol-2-yl-based ligands. The ambiphilic carbene (indol-2-yl carbon) of these complexes is extremely active and shows unique selective reactivity towards various organic molecules including carbodiimides, imine, diphenyldiazomethane, aluminum alkyls, 9-BBN and isonitriles, which demonstrate a range of unprecedented reactivity patterns such as formal [2 + 2] cyclometallation, [3 + 3] annulation, and aza-[4 + 1] annulation, while unprecedented aza-[4 + 1 + 1] annulation products were isolated from the reactions of the rare-earth metal complexes bearing electrophilic carbenes and strongly polarized metallacyclopropanes with 2,6-dimethylphenylisonitrile. Such reactivities differ sharply from those of common transition-metal complexes with the corresponding substrates. The electronic and steric effects of the ligands and the effects of central metal ions on the reactivity patterns were investigated both computationally and experimentally.

Introduction

The design and synthesis of new ligands for catalysis is among the ever-green research areas in modern chemistry.[1] Particularly, organometallic complexes containing pincer ligands are well known for their exceptional thermal stability, distinctive reactivity and wide applicability in catalysis.[2] The reactivity of pincer complexes can be manipulated through modulations of substituents on the donor groups or introduction of diverse connections between the central backbone and donor groups.[3] Thus, various symmetric pincer ligands bearing different backbones such as phenyl,[4] pyridyl,[5] pyrrolyl,[6] carbazolyl,[7] carbon or heteroatom-bridged diaryl[8] and all-carbon carbolong pincer ligands[9] have been developed. Our group has been engaged in the development of pincer-type rare-earth metal complexes featuring non-symmetric indol-2-yl-based ligands with development of new catalysis for the transformations of various organic molecules.[10] On the other hand, amidate metal complexes demonstrated distinctive reactivity and catalytic performance,[11] with applications in olefin polymerization,[12] copolymerization,[13] ester polymerization,[14] and alkene hydroamination.[15] Despite these advances, multi-chelated amidate pincer ligated complexes bearing both ambiphilic carbenes and nucleophilic alkyls have so far been unreported and their reactivity remains elusive.

Singlet carbenes in late transition-metal complexes are known to have lone pair electrons donated to the metal center and an empty p-orbital to accept d-electrons from the metal to form π-backbonding (Scheme 1).[16] A recent study indicated that the p-orbital receptor properties of these carbenes can be effectively harnessed.[17] Given that rare-earth metal ions have no d-electron to form π-backbonding, rare-earth metal complexes bearing such electrophilic carbenes might possess unique reactivity for application in catalysis and activation of small molecules. However, the synthesis of rare-earth metal electrophilic carbene complexes has just been realized until very recently, and 1,1-alkyl or 1,1-H(D) migratory reactions, and unique reactivity patterns towards pyridine derivatives were found with these complexes (Scheme 1).[11g,18,19] The chemistry of

[a]Key Laboratory of Functional Molecular Solids, Ministry of Education, Anhui Laboratory of Molecule-Based Materials, College of Chemistry and Materials Science, Anhui Normal University, Wuhu 241000, Anhui, P. R. China. E-mail: swwang@mail.ahnu.edu.cn

[b]Anhui Laboratory of Clean Catalytic Engineering, Anhui Laboratory of Functional Coordinated Complexes for Materials Chemistry and Application, College of Chemical and Environmental Engineering, Anhui Polytechnic University, Wuhu 241000, Anhui, P. R. China. E-mail: wsw@ahpu.edu.cn

[c]State Key Laboratory of Organometallic Chemistry, Shanghai Institute of Organic Chemistry, Chinese Academy of Sciences, Shanghai 200032, P. R. China

[d]LPCNO, CNRS & INSA, Université Paul Sabatier, 135 Avenue de Rangueil, 31077 Toulouse, France. E-mail: laurent.maron@irsamc.ups-tlse.fr

† Electronic supplementary information (ESI) available: CCDC 2258652–2258653, 2386247–2386289, 2258655, 2278784, 2278786 and 2278788. For ESI and crystallographic data in CIF or other electronic format see DOI: https://doi.org/10.1039/d5sc01502b

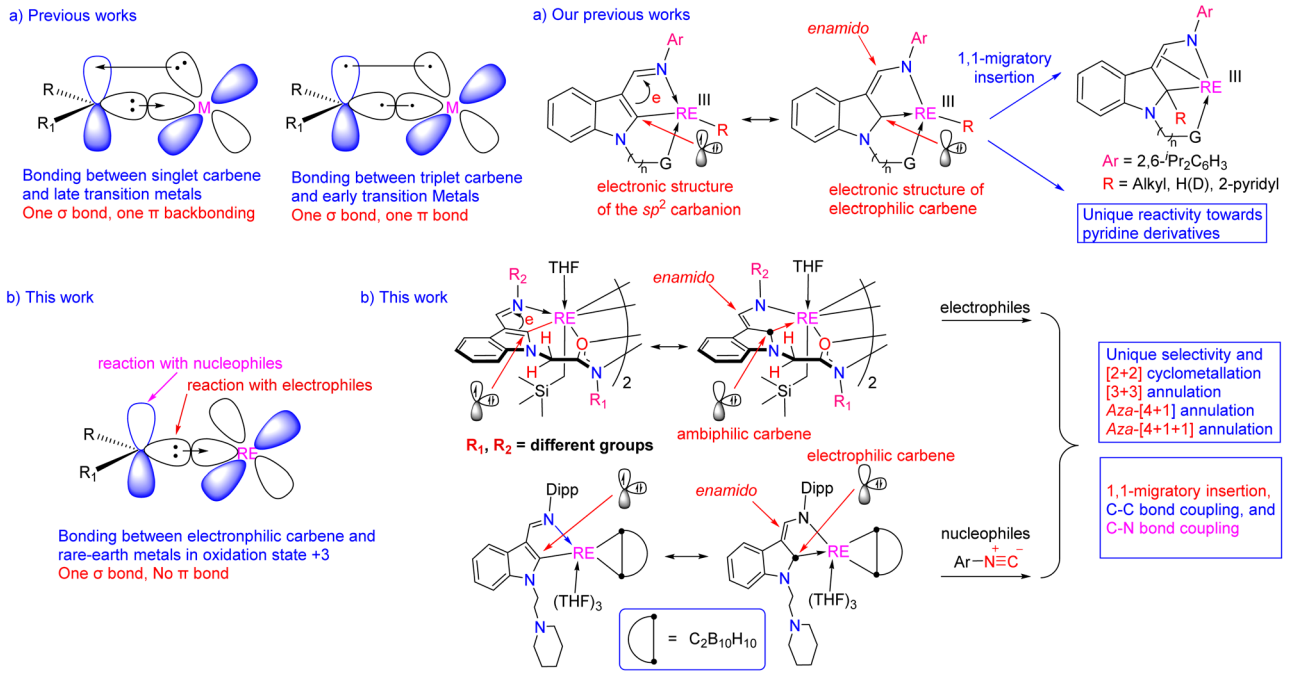

Scheme 1 Bonding and reactivity of the RE complexes bearing indol-2-yl ligands.

rare-earth metal complexes bearing an electrophilic carbene is far less developed in comparison with those of late transition metals.

N-Heterocyclic carbenes (NHCs) are one of the most widely used ligands and catalysts for their strong electron-donating and Lewis basic properties, as well as stable bonding with metals, and easy adjustment.[20] Cyclic (alkyl)(amino)carbenes (CAACs) are receiving extensive attention due to their ambiphilic character.[21] CAACs have also been applied in various fields such as transition-metal catalysis,[22] and light emitting materials as CAAC–Cu complexes.[23] Additionally, isolated CAACs have high thermal stability that can be utilized in stabilizing paramagnetic substances and activating small molecules (such as CO,[24] P_4,[25] H_2 (ref. 26) and NH_3 (ref. 26)). Following these pioneering studies of the CAACs, other types of ambiphilic carbenes have been developed and applied in catalysis or activation of small molecules.[27] However, these carbenes have only been used as supporting ligands in rare-earth metal chemistry, and studies on the chemistry of rare-earth metal complexes bearing both ambiphilic carbene and nucleophilic alkyl have to overcome some challenges including the lack of a model molecular platform due to their high activity and instability.

The reactions of isonitriles with transition metal compounds have been extensively studied with findings of cyclization reactions, migration insertion and multi-component reactions.[28] The insertion of isonitriles into the metal-element σ bond will result in the formation of complexes having η^1- or η^2-imidoyl (iminoacyl) (Scheme 2);[29] or the η^1 or η^2 formyl complexes;[30] or the bridged μ^2-CNR ligands. The insertion of isonitriles into the multiple M=C carbon bond will form metallacyclopropanes (η^2 ketenimine) or κ^1 ketenimine;[31,32] insertion of isonitrile into the Sc–C bond of aryl rare-earth metal complexes generates imidoyls, these complexes participate in

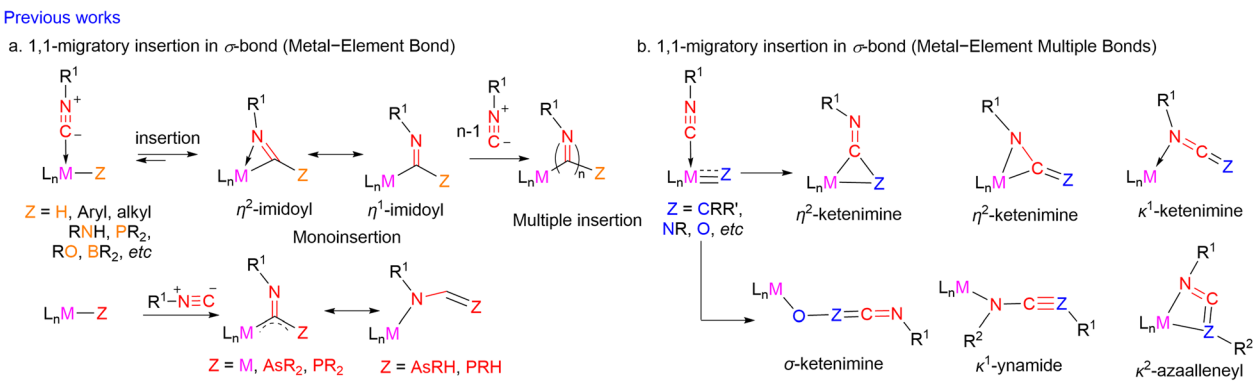

Scheme 2 Reaction modes of isonitrile with metal complexes.

further transformation reactions and then form an unusual indoline scandium with another isonitrile molecule.[32,33] These findings enrich the methods for constructing chemical bonds in organic synthesis. However, the reactivity pattern of rare-earth metal complexes having both ambiphilic carbenes and nucleophilic carbons with isonitriles remains elusive.

Herein, we report the design, synthesis and reactivity study of homodinuclear pincer-type rare-earth metal alkyl complexes featuring novel multi-chelated 1-amidate-3-imino functionalized indol-2-yl ligands, and reactivity study of rare-earth metal complexes bearing electrophilic carbon and strongly polarized metallacyclopropanes with 2,6-dimethylphenylisonitrile. The RE–$C_{carbene}$ bonds of these complexes exhibit unique selective reactivity towards electrophiles and nucleophiles, which could be associated with the ambiphilic carbene nature of the indol-2-yl carbon as revealed by DFT calculations and experimental results.

Results and discussion

Synthesis and characterization of multi-chelated amidate homodinuclear pincer rare-earth metal complexes bearing ambiphilic carbene and nucleophilic alkyl

The reactions of the ligand precursors H_2L^{Ad} [L^{Ad} = 1-[(*N*-2,6-$^iPr_2C_6H_3$)NCOCH$_2$]-3-($C_{10}H_{15}$N=CH)–C_8H_4N, Ad = adamantyl, $C_{10}H_{15}$]; H_2L^{Dipp} [L^{Dipp} = 1-[(*N*-2,6-$^iPr_2C_6H_3$)NCOCH$_2$]-3-(2,6-$^iPr_2C_6H_3$N=CH)–C_8H_4N; Dipp = 2,6-$^iPr_2C_6H_3$]; H_2L^{DMA} [L^{DMA} = 1-[(*N*,*N*-Me$_2$)NCOCH]-3-(2,6-$^iPr_2C_6H_3$N=CH)–C_8H_4N] (see the ESI†) with RE(CH_2SiMe_3)$_3$(THF)$_n$ (RE = Gd, Dy, Y, Er, Yb, Lu) in a 1 : 1 stoichiometric ratio at room temperature in tetrahydrofuran (THF) or toluene for 3 h produced the corresponding novel multi-chelated amidate homodinuclear pincer rare-earth metal complexes [η^1:η^1:(μ-η^1:η^2)-L^{Ad}RE(CH_2SiMe_3)(-THF)]$_2$ [RE = Gd(**1a**), Dy(**1b**), Y(**1c**), Er(**1d**), Yb(**1e**), Lu(**1f**)]; [η^1:η^1:(μ-η^1:η^2)-L^{Dipp}RE(CH_2SiMe_3)(THF)]$_2$ [RE = Y(**2a**), Er(**2b**), Yb(**2c**), Lu(**2d**)]; [η^1:η^1:(μ-η^1:η^2)-L^{DMA}RE(CH_2SiMe_3)(THF)]$_2$ [RE = Y(**3a**), Er(**3b**), Yb(**3c**), Lu(**3d**)] in high yields (Scheme 3, Fig. 1 and S52–S65 in the ESI†). All complexes were fully characterized by spectroscopic methods and elemental analyses, and their structures were confirmed by single-crystal X-ray diffraction.

The diamagnetic complexes **1c**, **1f**, **2a**, **2d**, **3a**, and **3d** were further characterized by NMR spectroscopy. In the ^{1}H NMR spectrum of complex **1c**, the signal centred at −0.23 ppm could be assigned to the resonances of the methylene protons of the CH_2SiMe_3 group, and is comparable with the resonance at −0.34 ppm (s, 2H) attributed to the protons of the methylene of the CH_2SiMe_3 in the 2-amidate indolyl yttrium complex.[4b] Unlike complex **1c**, the methylene protons of the Y–CH_2SiMe_3 in complex **2a** gave doublet resonances centred at −0.16 ppm ($^2J_{Y-H}$ = 8.0 Hz). Complex **3a** exhibits more pronounced coupling of yttrium ion nucleus with the protons of the CH_2SiMe_3, resulting in doublet resonances at −0.06 ppm ($^2J_{Y-H}$ = 15.0 Hz) and −0.16 ppm ($^2J_{Y-H}$ = 15.0 Hz). In addition, the corresponding methylene protons of the lutetium complexes were found to resonate at −0.37 ppm, −0.66 ppm (**1f**); −0.22 ppm, −0.37 ppm (**2d**); and −0.24 ppm, −0.32 ppm (**3d**), respectively, suggesting that the substituents of the ligands and coordinated THF might prevent the Lu–$C_{CH_2SiMe_3}$ bonds from free rotation, thus showing different proton resonances for the alkyls (–CH_2SiMe_3). The signal centred at 200.4 ppm in the $^{13}C\{^1H\}$ NMR spectrum of **1c** is attributed to the resonance of the carbon of the indol-2-yl coupled with the yttrium ion nucleus with $^1J_{Y-C}$ = 40.0 Hz, which can be compared with previously reported data.[10a,11g,18,19] The signal centred at 201.8 ppm assigned to the indol-2-yl carbon ($C_{2\text{-ind}}$) in the $^{13}C\{^1H\}$ spectrum of **2a** is coupled to the yttrium ion nucleus ($^1J_{Y-C}$ = 50.0 Hz), moving downfield as compared to that in **1c**. The signal centred at 201.3 ppm ($^1J_{Y-C}$ = 50.0 Hz) in the $^{13}C\{^1H\}$ spectrum of **3a** can be compared with the literature data (indol-2-yl carbon of L*RE(CH_2SiMe_3)$_2$(THF)$_x$ (L* = 1-(2-$C_4H_7OCH_2$)-3-(2,6-$^iPr_2C_6H_3$N=CH)C_8H_4N) at 201.8 ppm).[18] While the corresponding carbon resonances in the lutetium complexes **1f**, **2d**, **3d** shift even more downfield to 206.7, 209.2, and 210.9 ppm, respectively, these resonances for the indol-2-yl carbon atoms fall in the range of singlet metal carbenes.[34a]

X-ray analysis reveals that the amidates in complexes **1**, **2** and **3** adopt the μ-η^1:η^2 mode with the oxygen atoms of the amidates bridging two rare-earth metal ions; the amidates bond with one of the metal ions in η^2 mode, and the imino-functionalized indol-2-yl motifs bond with the central metal ions in

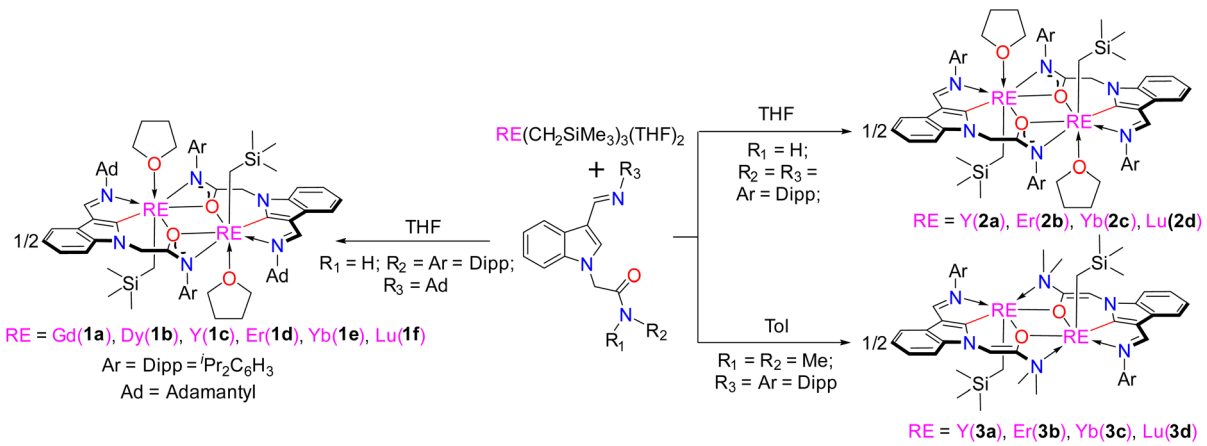

Scheme 3 Synthesis of the homodinuclear rare-earth metal alkyl complexes **1**–**3**.

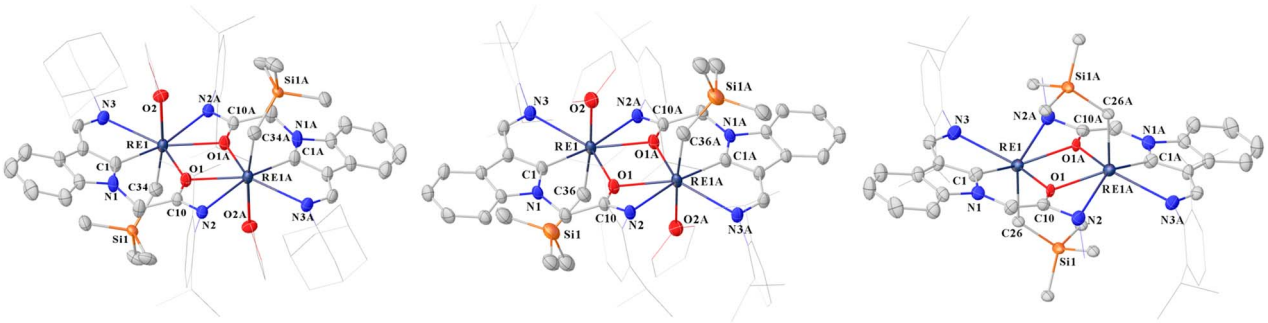

Fig. 1 Representative diagram for the complexes **1** (left), **2** (middle) and **3** (right) with thermal ellipsoids set at 30% probability level. All the hydrogen atoms are omitted, the diisopropylphenyl (Dipp) group and adamantyl (Ad) group are drawn in wireframe style for clarity. Selected bond lengths (Å) and selected bond angles (deg) can be read in the ESI.†

a manner of η^1:η^1. Thus, the bonding modes of the ligands with the central metal ions can be described as η^1:η^1:(μ-η^1:η^2) on the basis of analysis of the structural bond lengths (Tables S1–S3 in the ESI†). The indol-2-yl carbon atoms, imino, amidate groups and central metals are nearly coplanar in these rare-earth metal complexes. Obviously, two alkyl groups and two coordinated THF are present in the *trans*-form in complexes **1** and **2**. In the formation of complexes **1** and **2**, a sequence of indol-2-yl C–H activation and deprotonation is involved, while in the formation of complexes **3**, the activation of the indol-2-yl C–H and α C–H of the amide is involved to generate an amino-functionalized enolate anion bonding with the central metal ions in μ-η^1:η^2 modes. This difference highlights the influence of substituents on the reactivity of the ligand precursors with $RE(CH_2SiMe)_3(THF)_2$. It is found that the imino groups did not insert into the RE–C_{alkyl} bonds, which was different from previous results.[14] It's probably due to the stability of the multiple-chelated amidate pincer structure, the steric hindrance of the adamantyl or the aryl groups and electron isomerization resulting in the enamido motifs (Scheme 3). Unlike complexes **1** and **2**, the central metal ions in complexes **3** have six-coordination-number due to the absence of THF coordination, and the two alkyl groups present in the *trans*-form.

The bond lengths of RE1–$C_{2\text{-ind}}$, RE1–O1, RE1–N1, RE1–N3 and RE1–O1A in complexes **1a–1e**, **2a–2e** and **3a–3d** decrease with the decrease of ionic radius from Gd^{3+} to Lu^{3+} and Y^{3+} to Lu^{3+} (see Tables S1–S3 in the ESI†), which is consistent with the lanthanide contraction.[34b] The distances of RE1–$C_{2\text{-ind}}$ [2.388(5) Å for **1c**; 2.348(7) Å for **1d**; 2.351(6) Å for **1e**; 2.320(6) Å for **1f**] in complexes **1c–1f** are shorter than those of RE1–$C_{2\text{-ind}}$ [2.396(5) Å for **2a**; 2.367(3) Å for **2b**; 2.357(3) Å for **2c**; 2.335(3) Å for **2d**] of complexes **2a–2d**, probably due to the steric effects of the substituents on the ligands. The RE–$C_{2\text{-ind}}$ distances in **1** and **2** are shorter than those found in **L***$RE(CH_2SiMe_3)_2(THF)_x$ [(RE = Y, x = 1, 2.452(6) Å; RE = Er, x = 0, 2.387(4) Å; RE = Dy, x = 0, 2.396(3) Å; {**L*** = 1-(2-$C_4H_7OCH_2$)-3-(2,6-^{i}$Pr_2C_6H_3N$=CH)C_8H_4N}],[18] which can be attributed to coordination number and steric differences.

The O–C–N angles of the amidates range from 115.0(3)° to 117.3(6)° in complexes **1** and from 116.3(3)° to 116.8(4)° in complexes **2**. These data are very close to those (115.3(9)° to 119.3(11)°) in the amidate-functionalized N-heterocyclic carbene (NHC) rare-earth metal amido complexes.[34c] The N–C–O angles of the amidates (in the range of 107.7(4)° to 109.7(11)°) in complexes **3** are significantly smaller than the corresponding angles in complexes **1** and **2**, which can be attributed to the bonding differences between the amidate in **1** or **2** and the amino-functionalized enolate in **3**.

DFT calculations show that the indol-2-yl carbon atoms have a natural charge of −0.253 in **1c** and −0.260 in **2a**, which are substantially smaller than those of carbon atoms of the alkyl (–CH_2SiMe_3) (natural charge of −1.711 in **1c** and −1.716 in **2a**) in the corresponding complexes (Table 1). The natural charge of the indol-2-yl carbon atoms in complexes **1** and **2** can be compared with that of −0.228 found in **8a**, which bears strongly polarized carboryne-based metallacyclopropanes.[19b] This suggests some difference in reactivity and selectivity between the RE–$C_{2\text{-ind}}$ and RE–$C_{CH_2SiMe_3}$ bonds. The natural charges of

Table 1 Computed natural charges for **1c**, **2a** and **8a**

Atom label	Natural charges in **1c** (Y)	Natural charges in **2a** (Y)	Natural charges in **8a** (Y)[19b]
Y1	2.054	2.164	2.007
C1	−0.253	−0.260	−0.228
O1	−0.867	−0.901	−0.622(imino N)
O1A	−0.867	−0.901	−0.819(carboryne C)
N2A	−0.662	−0.681	−0.816(carboryne C)
N3	−0.654	−0.667	_
O2	−0.636	−0.665	_
C34 or C36	−1.711(C34 in **1c**)	−1.716(C36 in **2a**)	_

the indol-2-yl carbon atoms in the complexes **1c**, **2a** and **8a** are also smaller than those of the sp^2 carbanion (natural charge of −0.58) bonding with lutetium ion in the pentamethylcyclopentadienyl supported lutetacyclopropene, which displayed nucleophilic property according to the DFT calculations and experimental results.[35] The natural charges of the indol-2-yl carbon atoms in complexes **1c**, **2a** and **8a** are comparable to those in five-membered organometallic carbenes (ranging from −0.17 to −0.29 for different metals), which exhibit ambiphilic reactivity as indicated by the high values of protons and hydride affinities based on DFT calculations,[36] while the resonances for the indol-2-yl carbon atoms (see above) of these complexes can be compared with the resonances (~190–210 ppm) of the carbonyl carbon atoms of the ketones and aldehydes, which were generally accepted as electrophiles, demonstrating the electrophilic character of the indol-2-yl carbon atoms. Taken together, the indol-2-yl carbon atoms in these complexes can be described as ambiphilic carbon atoms.

Selective reactivity of the RE–$C_{2\text{-ind}}$ bond towards organic compounds containing electrophilic carbon or polar N=N double bond. Unusual [2 + 2] cyclometallation and [3 + 3] annulation

DFT calculations reveal that the natural charge of the indol-2-yl carbon of the complex **1c** is −0.25 (Table 1) and the natural charges of the carbon atoms of the alkyls (–CH_2SiMe_3) connected to the metal center are around −1.71, implying that these different RE–C bonds (RE–$C_{carbene}$ and RE–$C_{CH2SiMe3}$) may show different reactivities towards small organic molecules. To this end, the above-synthesized complexes **1** were subjected to reactions with a range of electrophiles (Scheme 4). Complexes **4a–4d** (Fig. S66–S69 in the ESI†) were crystallized from different solvents when 0.5 equiv. of complexes **1** were treated with carbodiimides or an aldimine. To our surprise, the RE–$C_{carbene}$ bonds selectively reacted with these electrophiles to generate novel [2 + 2] cyclometallation complexes **4a–4d**, in which the indol-2-yl carbon bonds with the central metal ions in η^1 mode (RE–$C_{2\text{-ind}}$ bond lengths: 2.803(4) Å in **4a**, 3.050(3) Å in **4b**, 3.062(3) Å in **4c**, 2.833(5) Å in **4d**, Scheme 4) due to the π-electron moving towards indol-2-yl carbon atoms after the reaction. In contrast, the RE–$C_{CH_2SiMe_3}$ bonds of the complexes **1**, which have the more nucleophilic carbon atoms as demonstrated by DFT calculations, did not react with the corresponding substrates, but reacted with the α C–H bond of the amidate to produce a novel amido-functionalized enolate functionality chelated with the central metal ions in μ-η^1:η^2 mode (complexes **4a–4d** in Scheme 4). These results are completely different from those of previous studies on the reactivities of rare-earth metal alkyls with carbodiimides and imine, which only produced the carbodiimides or imine insertion products with amidinate or amido being bonded with central metal ions in η^2 or σ bond ways.[37]

When complexes **1b** and **1e** were reacted with 4 equiv. of diphenyldiazomethane (Ph_2CN_2) at room temperature in THF for 0.5 h, complexes **4e** and **4f** were isolated (Fig. S70 and S71 in the ESI†). While treatment of **1b** with 4 equiv. of diphenyldiazomethane in THF overnight or standing the THF solution of **4e** overnight generated the product **4g** (Fig. S72 in the ESI†) *via* a rare formal [3 + 3] annulation (Schemes 3, 5 and Fig. 2). The formation of complex **4g** might involve a sequence of insertion of polar N=N bonds of the Ph_2CN_2 into RE–$C_{carbene}$ and RE–C_{alkyl} bonds to afford **4e**, activation of the α C–H bond of the

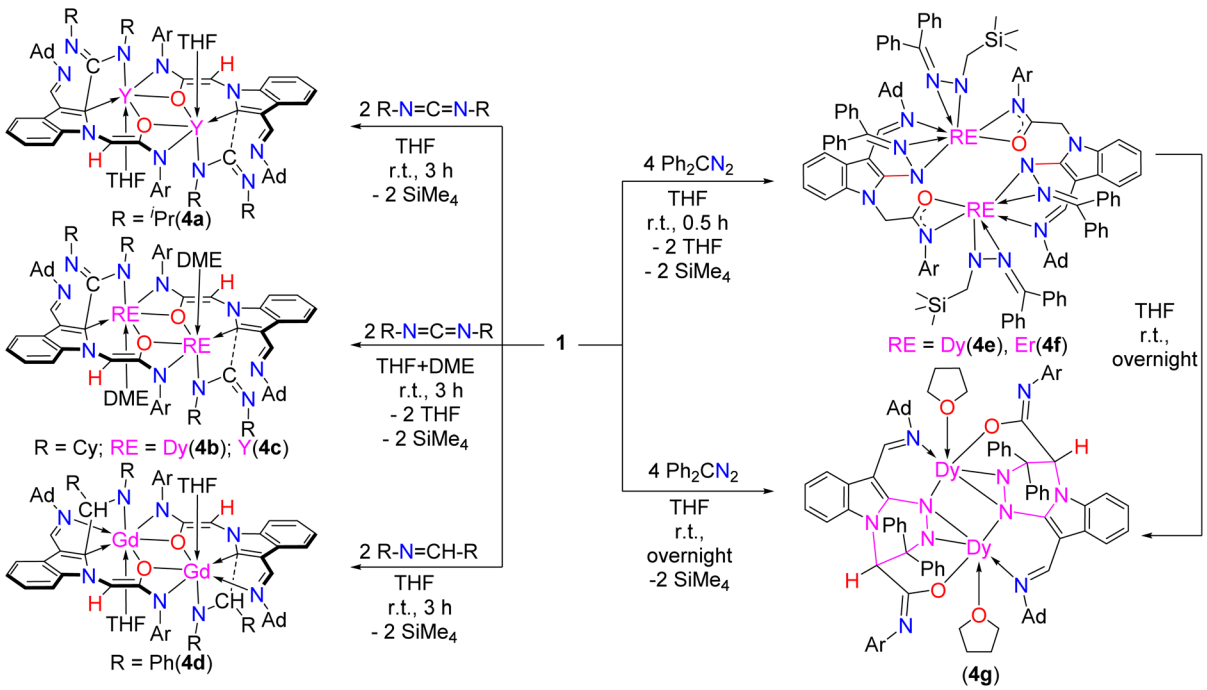

Scheme 4 The reactions of complexes **1** with electrophiles.

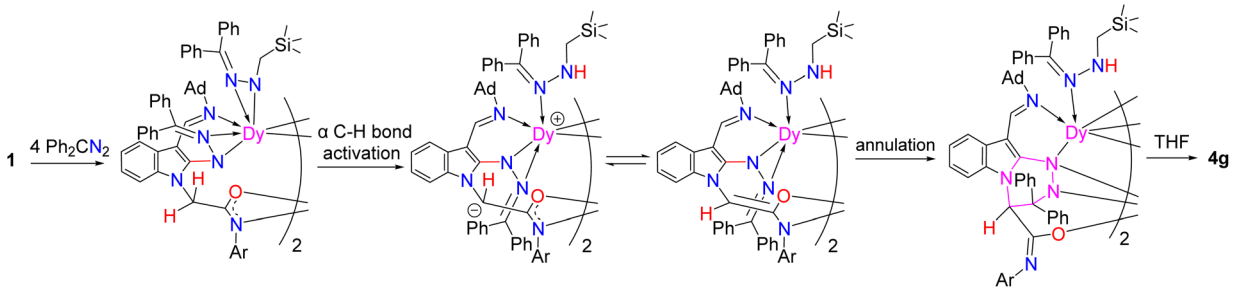

Scheme 5 A tentative pathway to complex **4g**.

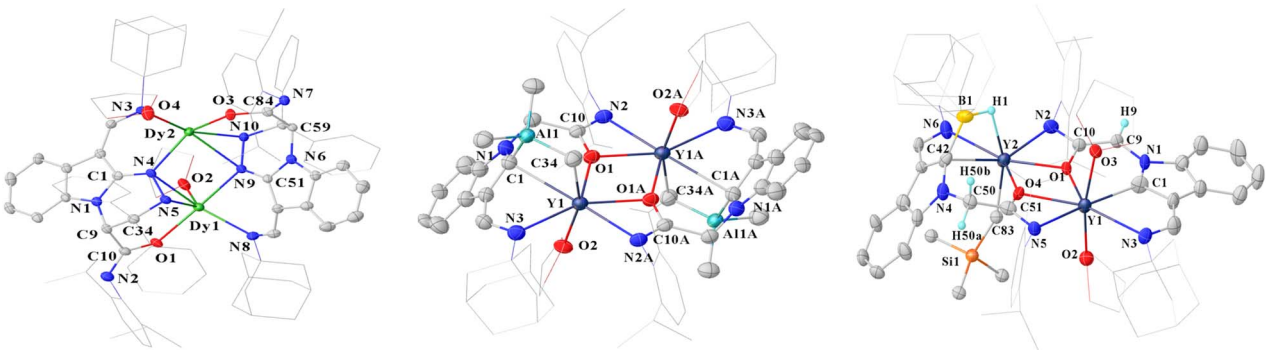

Fig. 2 Molecular structure of **4g** (left), **5c** (middle) and **5e** (right) with the thermal ellipsoid at 30% probability level. All hydrogen atoms were omitted and the diisopropylphenyl (Dipp) group was drawn in wireframe style for clarity. Selected bond lengths (Å) and selected bond angles (deg) can be read in the ESI.†

amidate by the anionic $[PhC{=}NNCH_2SiMe_3]^-$ to produce the amido-functionalized enolate and ring closure with C=N bond. The final step is accompanied by transformation of the amidate functionality into an imine functionalized alkoxide type motif.

Selective reactivity of complexes 1 with Lewis acids

To further probe the selective reactivity of the RE–$C_{carbene}$ bonds of complexes **1** towards electrophiles, we then tested their reactions with Lewis acidic compounds such as aluminum alkyls and 9-BBN (9-borabicyclo[3.3.1]nonane). It is interesting to find that the RE–$C_{carbene}$ bonds instead of the RE–$C_{CH2SiMe3}$ bonds, whose carbon has larger natural charge, of complex **1e** selectively reacted with the aluminum alkyls $AlMe_3$ and $AlEt_3$ to generate novel complexes **5a** and **5b** (Scheme 6, Fig. S73 and S74 in the ESI†). These complexes bear indol-2-Al_{alkyl} motifs with two sp^3 C–H bonds being σ donated to the ytterbium center, which is reduced to ytterbium(II) from ytterbium(III). Such a reduction is believed to proceed *via* the homolysis of the Yb–$C_{CH2SiMe3}$ bond[11g,38] due to its lower redox couple (−1.15 E_{295}/V) of Yb^{3+}/Yb^{2+}, which is supported by the identification of the coupling product $Me_3SiCH_2{-}CH_2SiMe_3$ (m/z = 174.126) from the reaction mixture. The reduction of ytterbium(III) to ytterbium(II) by the aluminum alkyls is occasionally proposed in the polymerization of olefins with mixed ytterbium complexes and aluminum alkyl catalytic systems to explain their poor catalytic activity compared with other rare-earth metal catalysts.[11d,f,39] However, the proposed ytterbium(II) intermediate has seldom been isolated and characterized. It is surprising to find that either the $AlMe_3$ or the $AlEt_3$ exists on the same side to the ytterbium metal in the solid state of the complexes **5a** and **5b**. Furthermore, the distances of 2.718(8) Å in **5a**, and 2.733(4) Å in **5b** of the sp^3 C–H interaction with the Yb metal are significantly shorter than that of 2.86 Å found in Sm^{II}–Me interaction in the bis(Me_3Si-fluorene-$AlMe_3$)Sm complex,[40] indicating strong σ donation in complexes **5a** and **5b**. This reactivity pattern is different from the reactions of $\mathbf{L}'Ln(CH_2C_6H_4NMe_2\text{-}o)_2$ ($\mathbf{L}'$ = $(PhCH_2)_2NC(NC_6H_3{}^iPr_2\text{-}2,6)_2$) with $AlMe_3$ or $AlEt_3$ producing the methyl bridged rare-earth metal–aluminum mixed metal complexes[41] or the ethylene and ethyne complexes.[42] The Al–$C_{2\text{-}ind}$ bond length (2.071(9) Å in **5a**, and 2.086(5) in **5b**) is within the expected range compared with Al–$C_{fluorenyl}$ (2.101(7) Å).[40] The average Yb^{II}–$C_{(CH_2)}$ bond length of 2.711 Å in 7-coordinate **5b** is longer than that found in 6-coordinate $Yb^{II}Al_2Et_8(THF)_2$ (2.633(2) Å),[43] which may be due to an electrostatic interaction.

When the rare-earth metal complexes **1b** and **1c** with the central metal having higher redox potential in comparison with Yb^{3+}/Yb^{2+} were treated sequentially with $AlMe_3$ and $(C_6F_5)_3B$, the cationic rare-earth metal complexes **5c** and **5d** were isolated from a mixed solution of *n*-hexane and chlorobenzene (Scheme 5, Fig. S75 and S76 in the ESI†). In this process, the RE–$C_{carbene}$ bond selectively reacts with $AlMe_3$ to deliver the indol-2-yl carbon connected aluminum intermediate, followed by activation of the C–H bond of the $AlMe_3$ to generate the rare hetero-rare-earth metal–aluminum four-membered metallacycles **5c**

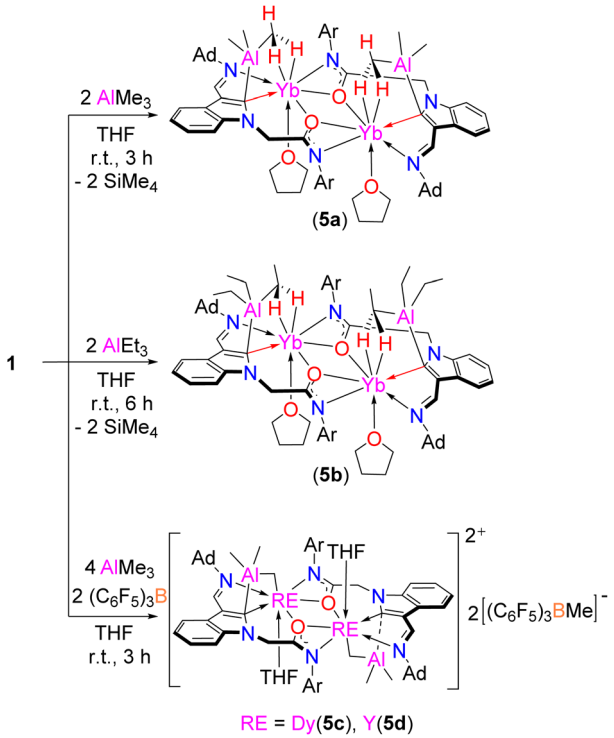

Scheme 6 The reactions of complexes **1** with AlR_3.

and **5d**. The RE–$C_{(CH_2)}$ bond lengths of 2.353(6) Å in **5c** and 2.356(5) Å in **5d** are comparable to the σ bond length of the Y–$C_{CH_2SiMe_3}$ in **1c**, and the Al–$C_{(CH_2)}$ bond lengths of 1.811(6) Å in **5c** and 1.809(5) Å in **5d** are shorter than that of 1.986(19) Å in **5a**. This reactivity pattern is different from those of the reactions of $\mathbf{L}'Ln(CH_2C_6H_4NMe_2\text{-}o)_2$ ($\mathbf{L}' = (PhCH_2)_2NC(NC_6H_3{}^iPr_2\text{-}2,6)_2$) with $AlMe_3$ producing the carbyne complex $[(PhCH_2)_2NC(NC_6H_3{}^iPr_2\text{-}2,6)_2]_2Y_2(\mu_2\text{-}Me)(AlMe_3)_2(\mu_4\text{-}CH)$ and alkyl abstraction product $AlMe_2(CH_2C_6H_4NMe_2\text{-}o)$ upon allowing the reaction mixture to stand for 7 days or running the reaction at 60 °C for 18 h.[41] In the present case, one methyl group was transferred to $(C_6F_5)_3B$ to produce the anionic $[(C_6F_5)_3BMe]^-$ part of the complexes, which are also different from the result of the reaction of $[(C_5Me_5)La(AlMe_4)_2]$ with $(C_6F_5)_3B$, which afforded a CH_3/C_6F_5 exchange product $[\{[(C_5Me_5)La\{(\mu\text{-}Me)_2AlMe(C_6F_5)\}][Me_2Al(C_6F_5)_2]\}_2]$.[44] The present results are also different from those of the reactions of aluminum alkyls with $B(C_6F_5)_3$ in ether solvent producing the borate $[Me_2Al(THF)_2]^+[MeB(C_6F_5)_3]^-$,[45] indicating electronic and steric effects of the ligands on the reactivity patterns.

Encouraged by the above results, the reactivity of complexes **1** with Lewis acidic 9-BBN has been investigated. A rare nonsymmetric dinuclear yttrium complex **5e** (Schemes 6 and 7, Fig. 2 and S77 in the ESI†) was obtained when complex **1c** was treated with 1 equiv. of 9-BBN at room temperature in THF. X-ray analysis reveals that complex **5e** is composed of a rare Y–$C_{2\text{–ind}}$–B–H four-membered bora-metallacycle with the indol-2-yl carbon bonding to the metal in the η^1 way. The formation of **5e** might involve selective reaction of the Y–$C_{carbene}$ bond with 9-BBN, while the Y–CH_2SiMe_3 bond of which the carbon has

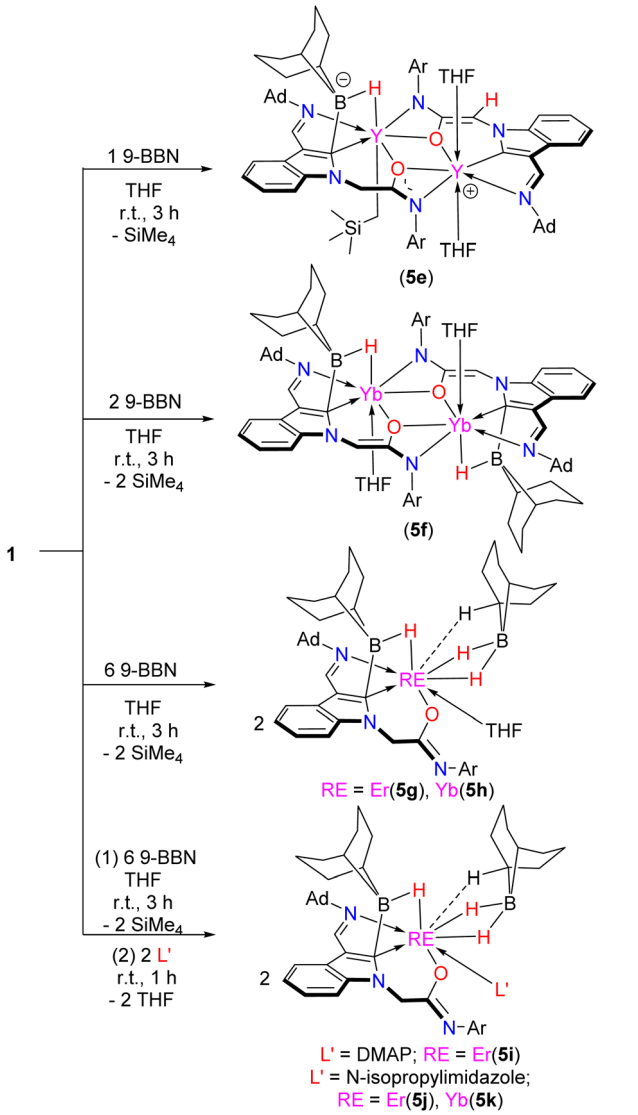

Scheme 7 The reactions of complexes **1** with 9-BBN.

larger natural charge remains intact. Complex **5e** contains a unique multi-chelate amidate pincer ligand bearing a four-membered bora-metallacycle with the indol-2-yl carbon bonding to the metal centre in the η^1 way in one part, and a multi-chelate amido-functionalized enolate pincer ligand in the other part (Schemes 7 and 8). The Y(2)–$C(42)_{2\text{-ind}}$ bond length (2.741(9) Å) is significantly longer than Y(1)–$C(1)_{2\text{-ind}}$ (2.381(10) Å). This suggests that the RE–$C(42)_{2\text{-ind}}$ bond might have transformed from the σ bond into the π bond (η^1) way due to the electron-deficient bora functionality to make the π-electron of the ligand move towards the indol-2-yl carbon (Scheme 1). The Y–H bond length (2.3817(11) Å) was slightly long with those of the Sc–H (borate bridged) (Sc–H = 2.01(3) Å and 2.11(2) Å) when the ionic radii differences were taken into account.[46] The reaction of complex **1e** with 2 equiv. of 9-BBN in THF leads to the isolation of the central symmetric dinuclear complex **5f** bearing a four-membered bora-metallacycle with the indol-2-yl carbon being η^1 bonded (Yb–$C_{2\text{-ind}}$ bond length 2.650(7) Å) to

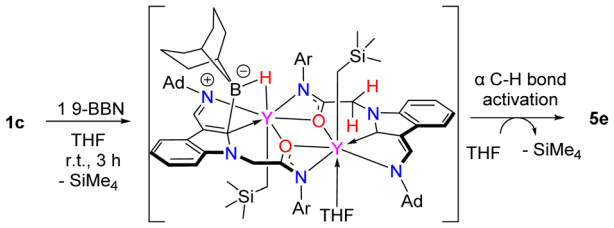

Scheme 8 The formation process of complex **5e**.

the metal centres (Scheme 7 and Fig. S78 in the ESI†). The formation of **5f** is believed to go through selective reaction of the Yb–$C_{2\text{-ind}}$ bond with 9-BBN to afford the 2-borate indolyl, and the Yb–CH_2SiMe_3 bond activates the α C–H of the amidate group to generate the multi-chelate amido-functionalized enolate 2-borate indol-2-yl ligated dinuclear complex. It is noted that while the four-membered bora-metallacycle has been proposed as an intermediate in the metathesis reactions of the RE–C bond with hydroborate or 9-BBN in the catalytic hydroboration of unsaturated compounds,[47] to date, structural information about this kind of four-membered ring is rare.

Interestingly, when complexes **1** were treated with excess 9-BBN (6 equiv.) in THF, the THF coordinated mononuclear 2-borate indolyl supported and 9-BBN bridged rare-earth metal hydrides **5g** and **5h** were isolated (Scheme 7 and Fig. S79–S80 in the ESI†). Stepwise reactions of complexes **1** with excess 9-BBN in THF followed by treatment with donor molecules such as 4-*N*,*N*-dimethylaminopyridine (DMAP) or *N*-isopropylimidazole (IPIMD) provide DMAP- and IPIMD-coordinated complexes **5i–5k** (Scheme 7 and Fig. S81–S83 in the ESI†). Similar to the formation of complexes **5e** and **5f**, the RE–$C_{carbene}$ bond selectively reacted with 9-BBN first, and then the RE–C_{alkyl} bond reacted with another equivalent of 9-BBN to split the dinuclear complexes into mononuclear ones. An electrostatic C–H interaction (RE–H bond distances 1.976(13) Å to 2.439(18) Å) of the 9-BBN with the rare-earth metal center was found. It is interesting to find that the amidate transforms into the imino-functionalized alkoxide form. This prevents the α C–H of the original amidate from being activated by either the RE–CH_2-$SiMe_3$ or the newly generated RE–H bonds to generate the amido-functinonalized enolate, which is different from the formation of **5e** and **5f**. The indol-2-yl carbon bonds with the central metal ion in the η^1 way due to the electron-deficient bora functionality to make the π-electron of the ligand move towards the carbon. The RE–H bond distances found in **5g** and **5h** (Scheme 7) can be compared to those found in the divalent ytterbium and europium 9-BBN complexes, $(THF)_4Yb[(\mu\text{-}H)_2BC_8H_{14}]_2$, and $(THF)_4Eu[(\mu\text{-}H)_2BC_8H_{14}]_2$,[48a] the trivalent yttrium tetrahydroborate, $(MeOCH_2CH_2C_5H_4)_2Y[(\mu\text{-}H)_2BH_2]$,[48b] and $(C_5Me_5)_2Y(\mu\text{-}H)_2BC_8H_{14}$.[48c] It is noted that the α C–H activation has not been found in the formation of **5i–5k** with the addition of 4-*N*,*N*-dimethylaminopyridine (DMAP) or *N*-isopropylimidazole (IPIMD), which is different from the previous reports.[11g]

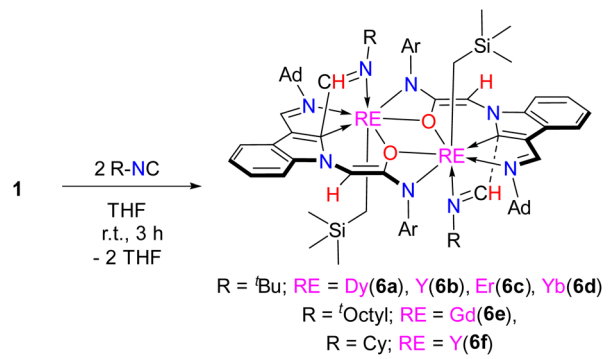

Scheme 9 The reactions of complexes **1** with isonitriles.

Selective reactions of the complexes with isonitriles. Unique selectivity and ligand effects on the reactivity patterns

The above results of reactions of the synthesized complexes with electrophiles prompted us to investigate the reactivity of these complexes towards nucleophiles such as isonitriles. It is unexpectedly found that the *tert*-butylisonitrile (^{t}BuNC, 2 equiv.) is selectively reacted with carbene carbon atoms (indol-2-yl carbon atoms) of the complexes **1** in THF at ambient temperature, complexes **6a–6d** are generated in good yields, and the highly polarized RE–$C_{CH2SiMe3}$ bonds remain intact (Scheme 9, Fig. 3 and Fig. S84–S87 in the ESI†). X-ray crystallography

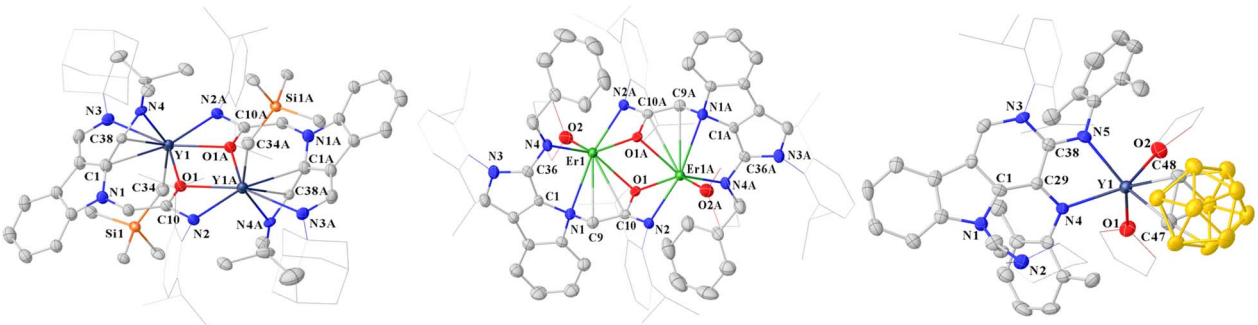

Fig. 3 Molecular structure of **6b** (left), **7d** (middle) and **9a** (right) with the thermal ellipsoid at 30% probability level. All hydrogen atoms were omitted and the diisopropylphenyl (Dipp) group was drawn in wireframe style for clarity. Selected bond lengths (Å) and selected bond angles (deg) can be read in the ESI.†

confirms that complexes **6a–6d** contain the aza-metallacyclobutene motifs with the Y–$C_{2\text{-ind}}$ distance of 2.757(6) Å, $C_{2\text{-ind}}$–C_{imino} bond length of 1.510(10) Å, and Y–N4 bond length of 2.459(6) Å. The N4–C38 distance of 1.385(10) Å reveals a C=N double bond character. Complexes **6a–6d** cannot undergo further insertion reaction or C–C coupling in the presence of an excess of ^{t}BuNC (>2 equiv.) under the reaction conditions. When other isonitriles such as *tert*-octylisonitile and cyclohexylisonitrile were used, the corresponding rare-earth metal complexes **6e** and **6f** (Scheme 9, Fig. S88 and S89 in the ESI†) containing the aza-metallacyclobutene moiety were also isolated, and the RE–$C_{CH2SiMe3}$ bonds remained unreacted. This reactivity pattern is consistent with the electrophilic nature of the indol-2-yl carbon as revealed by DFT calculations (Table 1). However, aryl isonitriles seem incompatible in this reaction system in that the reaction of 2,6-dimethylphenylisonitrile (XylNC) with complex **1f** gave an unidentifiable mixture.

It is proposed that the formation of complexes **6** involves coordination of isonitrile to the electrophilic metal centre with the release of THF to afford the intermediate ^{Ad}Y1, which then undergoes 1,1-migratory insertion to the electrophilic indol-2-yl carbene carbon[18,19a,c] to produce the intermediate ^{Ad}Y2. The Y–$C_{2\text{-ind}}$ bond cleavage occurs with intramolecular redox to afford the intermediate ^{Ad}Y3, which then abstracts the proton of the α C–H of the amidate group to deliver the final product (Scheme S30 in the ESI†). This reactivity pattern is different from the known reaction of a free singlet carbene with an isonitrile to generate a ketenimine.[49] To the best of our knowledge, the selectivity and reactivity found in the above reactions have so far been unreported.[50] It is noteworthy that the Y–N4 bonds (2.459(6) Å) in **6b** are significantly longer than those in the $[(C_5H_5)Y(\mu,\eta^2\text{-HC=NCMe}_3)]_2$ dimer (2.325(4) Å),[51a] and in the $Cp^*_2Zr(iminoacyl)CH_3$($Cp^* = C_{10}H_{15}$) monomer (2.368(2) Å)[51b] respectively, due to different coordination numbers and/or different central metal ions.

Next, taking the reaction of **1c** with ^{t}BuNC to produce **6b** as an example, DFT calculations were performed to investigate the possible reaction pathways and reasonable energy profiles (see the ESI† for details). The results showed that the total reaction was exergonic −42.4 kcal mol^{-1}, and the reaction barriers were consistent with room temperature conditions. The formation of complex **6b** might proceed *via* a stepwise process at each metal

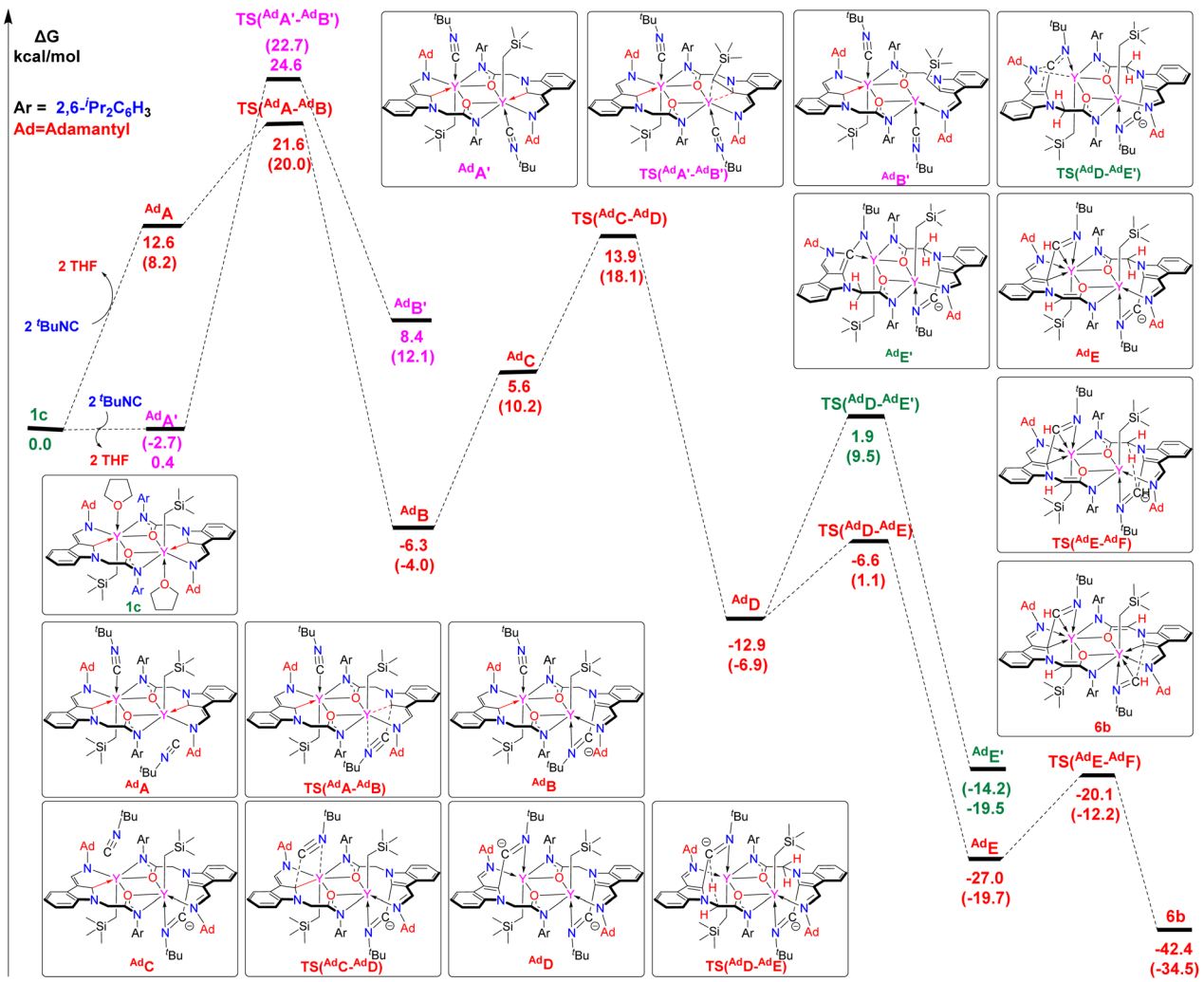

Scheme 10 Computed enthalpy profile for the formation of **6b** from **1c**. The enthalpy is given in kcal mol^{-1}.

centre to accomplish the formation of the aza-metallacyclobutene moiety. After coordination of the ^{t}BuNC, the 1,1-^{t}BuNC migratory insertion accompanied by Y–$C_{2\text{-ind}}$ cleavage leads to the reduction of isonitrile C≡N triple bond to the imidoyl anion (intramolecular redox). This process is preferred to the 1,1-CH_2SiMe_3 migratory insertion with a formation of relatively stable intermediate ^{Ad}**B** (−6.3 kcal mol^{-1}) *vs.* ^{Ad}**B**′ (8.4 kcal mol^{-1}). The intermediate ^{Ad}**B** transforms into the intermediate ^{Ad}**C** (5.6 kcal mol^{-1}), which then undergoes another 1,1-^{t}BuNC migratory insertion accompanied by Y–$C_{2\text{-ind}}$ cleavage leading to reduction of isonitrile C≡N triple bond to generate the intermediate ^{Ad}D (−12.9 kcal mol^{-1}). The process of abstraction of the α C–H of the amidate group to form intermediate ^{Ad}**E** (−27.0 kcal mol^{-1}) is favourable to the cycloaddition of the imino nitrogen of the ligand to the ketenimine carbon. The ^{Ad}**E** then abstracts another proton of the α C–H of the amidate group to deliver the final product **6b** (−42.4 kcal mol^{-1}) (Scheme 10).

To get more direct information of the substituent effects on the reactivity, we then investigated the reactivity of different complexes towards various isonitriles. It is surprising to find that when complexes **2** bearing the ligand with a diisopropylphenyl substituent instead of the adamantyl substituent in **1** were treated with different isonitriles (R–NC, R = ^{t}Bu, ^{t}Octyl, Bn, Xyl) under the otherwise same conditions, novel [4 + 1] annulation products of 1-amido-functionalized enolate indolo-fused 2-amido-pyrrolyl complexes **7** (Scheme 11, Fig. 3, and S90–S95 in the ESI†) were isolated with moderate yields. In this process, the carbene carbon atoms (indol-2-yl carbon atoms) have displayed unexpected selective reactivity towards the nucleophilic isonitriles, which is completely different from that found in reactions of **1** with isonitriles. This suggests that the substituents on the ligand, which may lead to changes in both steric hindrance and electronic nature of complexes **1** and **2** (different natural charges of the central metal ion and the bonding atoms, see Table 1), have profound effects on the reaction pathways. The current results with isonitriles are also completely different from those in recently reported reactions of rare-earth metal monoalkyl complexes with isonitriles, which provided multi-substituted β-diketiminato or multi-substituted imidazolyl complexes.[52] On the basis of the DFT calculation results, it is proposed that coordination of the isonitrile to complex **7a** (as an example) gives the intermediate ^{Dipp}Y1, which then undergoes 1,1-migratory insertion to generate ^{Dipp}Y2. Isomerization of ^{Dipp}Y2 gives the ketenimine[49] intermediate ^{Dipp}Y3. Then the amido nitrogen of the ligand attacks the central carbon of the ketenimine to finish the cyclization to form the [4 + 1] annulation products of indolo-fused 2-amido pyrrolyl fragments ^{Dipp}Y4. The RE–$C_{CH_2SiMe_3}$ bonds activate the α C–H bonds of the amidate to deliver the final 1-amido functionalized enolate chelate indolo-fused 2-amido-pyrrolyl ligated complexes (Schemes 12 and S31 in the ESI†).

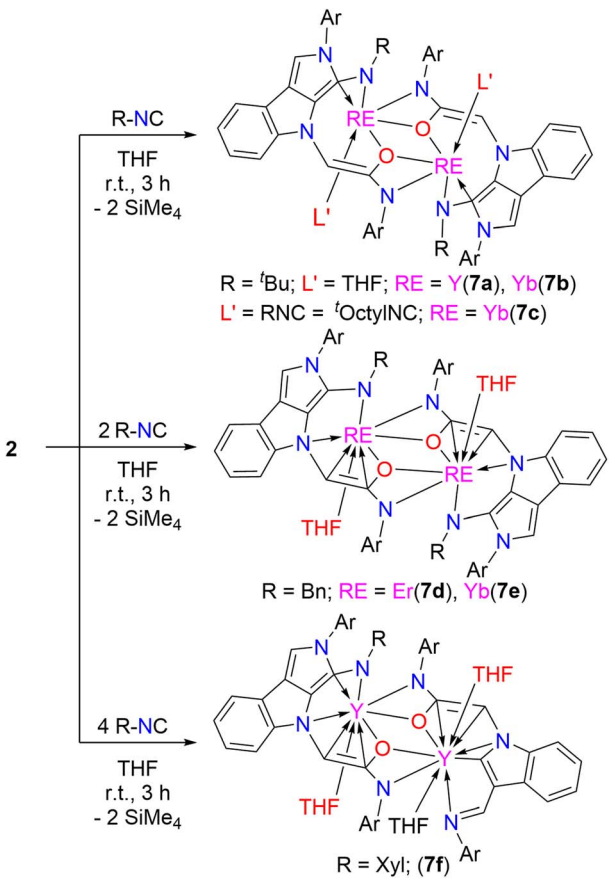

Scheme 11 The reactions of complexes **2** with isonitriles.

It should be noted that when complexes **2** were directly treated with excess *tert*-octylisonitrile (^{t}OctylNC) (4 equiv.), the C–C coupling or C–N coupling products through insertion of RN≡C to the RE–$C_{CH_2SiMe_3}$ bonds or through insertion of RN≡C to the RE–N bonds as those reported in the literature were not obtained,[51,53] while the ^{t}OctylNC coordinated complex **7c** was isolated instead. Also of note is that the original bonding modes of the ligand change from η^1:η^1:(μ-η^1:η^2) to σ:η^1:(μ-η^1:η^2) after the cyclization, that is, the newly generated amido-functionalized pyrrolyls bond with the central metal in σ:η^1 (RE–$C_{2\text{-pyr}}$: 2.669(13) Å to 2.793(13) Å) and the amido-functionalized enolates bond with the central metal in μ-η^1:η^2 ways in complexes **7a–7c**. When the substituents of isonitriles are benzyl or xyl (**7d–7f**), the reactions are compatible with these substrates, which are different from that of reaction of **1** with the xyl substituted isonitrile. It is found that the C=C double bonds of the newly formed amido-functionalized enolates in **7d–7f** have bonding interaction with the central metal as indicated by the RE–C bond distances of 2.685(7) Å to 2.715(5) Å.

In order to further understand the reaction process, the formation of complex **7a** from the reaction of complex **2a** with ^{t}BuNC was calculated by DFT (Scheme 12, see the ESI† for details). It reveals that the replacement of THF by ^{t}BuNC, followed by a stepwise 1,1-migratory insertion on each metal centre to generate the intermediate ^{Dipp}**D** are parallel to those for the formation of **6b** as discussed above. The transformation of ^{Dipp}**D** into the indolo-fused amido-functionalized pyrrolyl motif (^{Dipp}**E**) is favoured over the transformation of ^{Dipp}**D** into aza-metallacyclobutene (^{Dipp}**E**′) (4.0 kcal mol^{-1} *vs.* 4.6 kcal mol^{-1}). The intermediate ^{Dipp}**E** then undergoes a stepwise C–H activation with the RE–CH_2SiMe_3 bond followed by

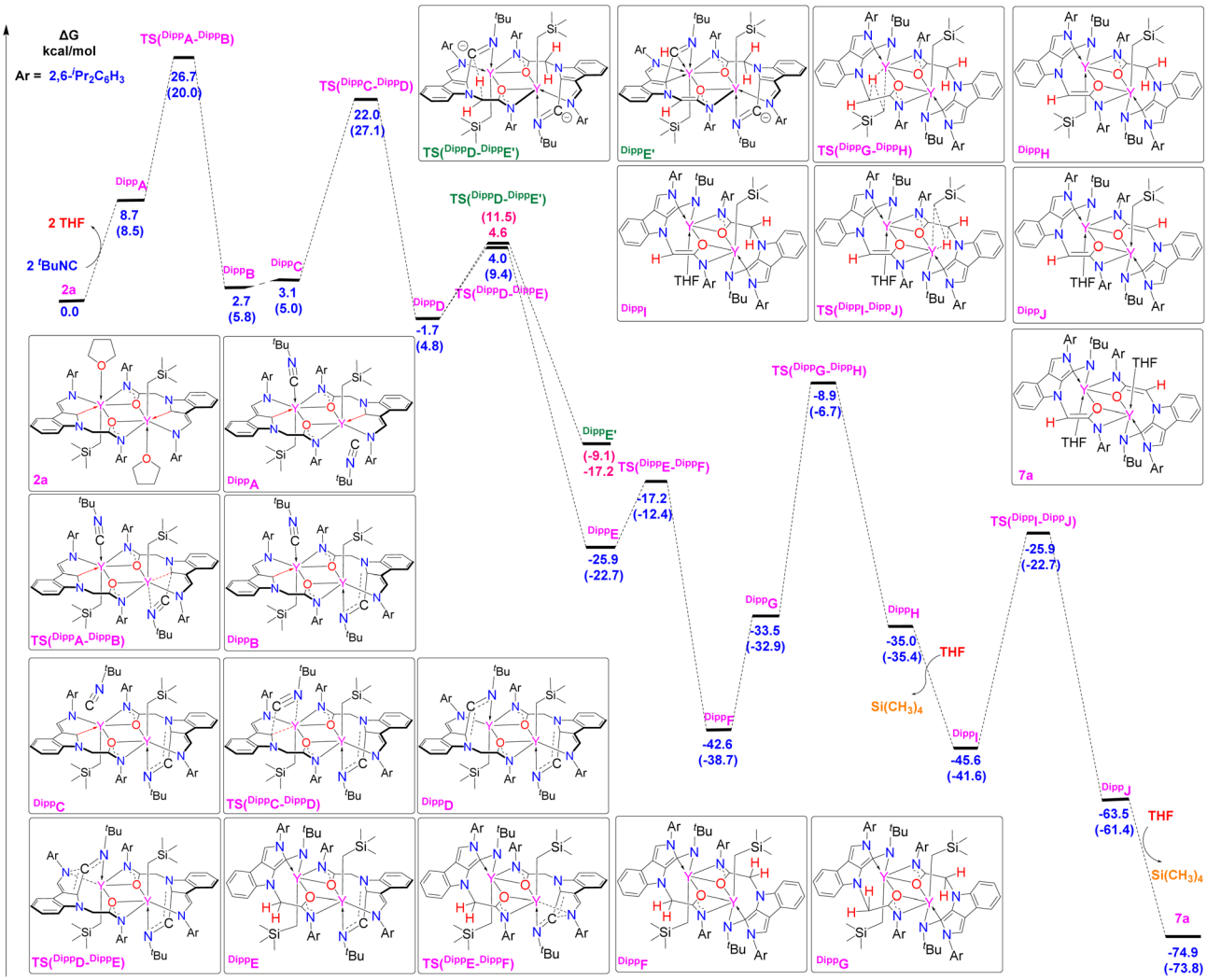

Scheme 12 Computed enthalpy profile for the formation of **7a** from **2a**. The enthalpy is given in kcal mol^{-1}.

coordination of THF to deliver the final products. These results suggest that the substituents on the ligands have influence on the electronic properties of the complexes and stability of the transition state and intermediates, thereby determining the reaction pathways of the complexes.

To prove the above results that ligands have profound influences on the reactivity patterns of rare-earth metal complexes with isonitriles, we then studied the reactivity of the rare-earth metal complexes bearing both electrophilic carbene and strongly polarized three-membered metallacycles with isonitrile. Treatment of the carboryne-based strongly polarized metallacyclopropane (κ^2-**L**^{1})RE(η^2-$C_2B_{10}H_{10}$)(THF)$_3$ [**L**^{1} = 1-(2-*N*-$C_5H_{10}NCH_2CH_2$)-3-(2,6-^{i}Pr$_2$C$_6$H$_3$N=CH)-C_8H_4N, RE = Y(**8a**), Er(**8b**), Lu(**8c**)][19b] with 3 equiv. of XylNC afforded the

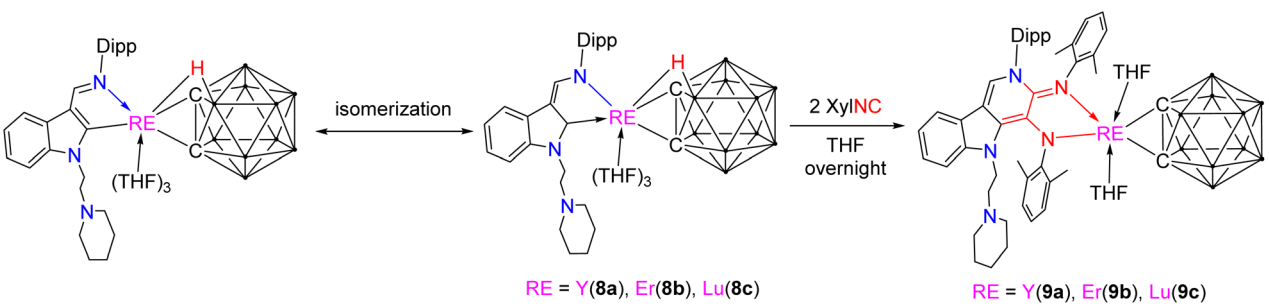

Scheme 13 Reactions of the indol-2-yl rare-earth metal carboryne-based metallacyclopropanes with XylNC.

unprecedented selective reaction complexes **9** bearing an α,β-di(2,6-dimethylphenyl)amido-γ-(*N*-2,6-diisopropylphenyl)carboline (or indolo-fused multi-functionalized pyridine)-based ligand (Scheme 13, Fig. 3 and S96–S98 in the ESI†). It is surprising to find that the highly strained and polarized metallacyclopropane moiety remains intact in the process, while the formation of the indolo-fused multi-functionalized pyridine moiety involves the coupling of the electrophilic carbene carbon and the nucleophilic nitrogen atom of the ligand (1-(2-C_5H_{10}-NCH_2CH_2)-3-(2,6-$^iPr_2C_6H_3NCH$)-C_8H_4N)-2-yl with two molecules of 2,6-dimethylphenylisonitrile *via* an unexpected aza-[4 + 1 + 1] annulation, which is obviously different from the reactivity of the zirconium–carboryne complex with isonitrile to produce the zirconium complex having the [^{t}BuN=C=C]$^-$ ketenimine moiety functionalized carborane anion through the insertion of isonitrile into the Zr–C_{cage} bond accompanied by the Zr–C_{cage} bond cleavage.[19b] The result is also different from those of the reactions of lutetium metallacyclopropene with phenylnitrile followed by treatment with 2,6-dimethylphenylisonitrile to produce the functionalized pyrrolyl moiety complex.[35] This result is also obviously different from the reactions of the rare-earth metal complexes **1** and **2** with isonitriles to generate the multi-substituted aza-[4 + 1] annulation and the [2 + 2] cyclometallation products as discussed above. These differences in reactivity patterns towards isonitriles may probably be due to ligands, central metal ions, coordination environments around the central metals, and electrophilic property of the indol-2-yl carbon atoms (comparison of the natural charge of the carbon about −0.253 in **1c** and −0.260 in **2a** with −0.228 in the corresponding carboryne-based yttrium metallacycle **8a**, see Table 1). It is found that the average lengths of the RE–C_{cage} bond in **9** are shorter than those of the corresponding rare-earth metallacyclopropane complexes (κ^2-L^1)RE(η^2-$C_2B_{10}H_{10}$)$(THF)_3$, which may be attributed to the difference in ionic radii between the different coordination numbers in complexes (κ^2-L^1)RE(η^2-$C_2B_{10}H_{10}$)$(THF)_3$. It is noted that the coupling of the imino nitrogen atom with unsaturated substrates is only involved in the aza-Diels–Alder reactions, where the imine nitrogen generally bears electron-withdrawing groups.

DFT calculations of complexes (κ^2-**L**^{1})RE(η^2-$C_2B_{10}H_{10}$)$(THF)_3$ (RE = Y, Lu) showed that the natural charges of the indol-2-yl carbon are −0.228 in yttrium and −0.213 in lutetium complexes,[19b] which are comparable with those found in complexes **1** and **2**, indicating that the indol-2-yl carbon is an electrophilic carbon because the corresponding p-orbital lacks electrons. These results are parallel to our previous findings of the indol-2-yl carbon which exhibited electrophilic property to make the 1,1-alkyl and 1,1-H (or D) migratory insertion possible,[18,19a] and findings of unique reactivity patterns towards pyridine derivatives.[19c] Based on these results, the formation of the γ-carboline-based α,β-diamido moiety functionalized complexes could be described as follows: complex (κ^2-L^1)Y(η^2-$C_2B_{10}H_{10}$)$(THF)_3$ was transformed into the intermediate **A** through ligand substitution, in which the indol-2-yl carbon is more electrophilic than that in (κ^2-**L**^{1})Y(η^2-$C_2B_{10}H_{10}$)$(THF)_3$ (natural charge: −0.132 in **A** *vs.* −0.228 in (κ^2-**L**^{1})Y(η^2-$C_2B_{10}H_{10}$)$(THF)_3$, Table S29 in the ESI†). The migratory insertion of the polarized coordinated isonitrile to the enamido-functionalized carbene with Y–$C_{carbene}$ bond cleavage produced the ketenimine intermediate **B**, which has been found in the reaction of free singlet carbene with isonitrile,[49] and is parallel to the above results of reactions of complexes **2** with isonitriles delivering intermediate ^{dipp}**D**. Then **B** underwent isomerization from *cis*-coordinated isonitrile to *trans*-coordinated isonitrile to give the ketenimine intermediate **C**, which then reacted with the coordinated isonitrile through insertion to afford the ketenimine intermediate **D** of the five-membered metallacycle. The difference in reactivity between the above formed rare-earth metal ketenimine intermediate and the present rare-earth metal ketenimine intermediate in the reactions with isonitriles can be attributed to the existence of the electrophilic carboryne motif, which may make the central carbon of the ketenimine more electrophilic, thereby allowing the coordinated isonitrile to attach to it easily. The amido group of the enamido functionality attached the carbon of the C=N double bond to produce the γ-carboline-based α,β-amidoimino moiety **E**, which then coordinates with two molecules of THF with release of one isonitrile to produce the final product **9a** (Scheme 14).

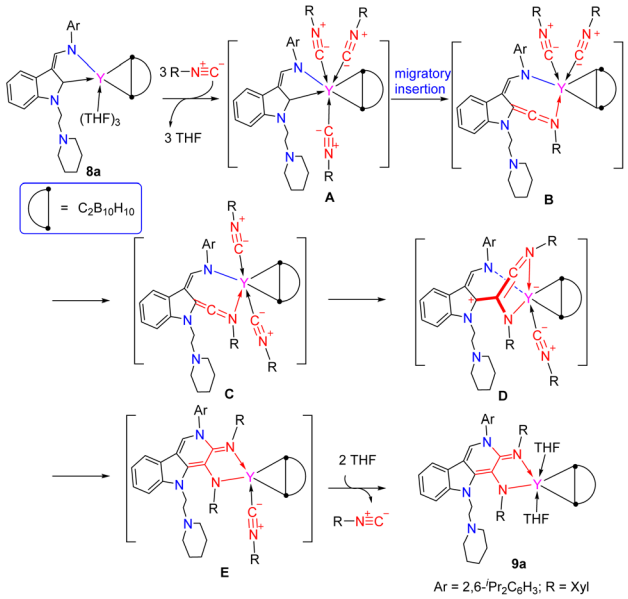

Scheme 14 A possible reaction pathway for the reaction of indolyl rare-earth carboryne-based metallacyclopropanes with XylNC.

To gain some insights into the formation of complex **9a** from complex **8a**, the computational studies were carried out at the level of B3PW91 including dispersion corrections (see the ESI† for details). The first step of the reaction is the formation of an yttrium centre with three coordinated isonitrile molecules, which will give a more stable **A** with corresponding indol-2-yl carbon which is more electrophilic (natural charge from −0.228 to −0.132). Two isomers were found (namely **A** and **A′** in Scheme S32 in the ESI†) that would allow two different reactivities. The most stable isomer is **A** which is 4.8 kcal mol^{-1} more stable than **A′**, so that the latter will never be formed, preventing the red

pathway in Scheme S32 in the ESI.† The red pathway, although kinetically accessible (barrier of 18.1 kcal mol^{-1}), is the insertion of isonitrile into the Y–C_{cage} bond, while the black pathway, which is kinetically competitive (within the precision of the computational method) with the red pathway (barrier of 23.3 kcal mol^{-1}), is the insertion into the Y–$C_{carbene}$ bond. Following the intrinsic reaction coordinates for both pathways, it yields complex **B′** and **C** where the latter is more stable than the former by 2.7 kcal mol^{-1} so that only complex **C** will be observed. This completely ruled out the reaction of isonitrile with the Y–C_{cage} bond. Complex **C** is an amido complex bearing a C=C=N group which is reminiscent of an anionic aza-allyl group. This C=C=N cumulenic ketenimine system contains a central sp-hybridized carbon atom that is electron-deficient. Thus, a second molecule of isonitrile undergoes a nucleophilic addition to the central carbon of the ketenimine at TS2 with an associated barrier of 20.8 kcal mol^{-1}. Following the intrinsic reaction coordinate, it yields another stable ketenimine intermediate **D** (−23.9 kcal mol^{-1}), which readily isomerizes through a ring closure reaction of the nucleophilic addition of the Y–N bond to the central carbon of the ketenimine (TS3). The associated barrier of this last step is 16.4 kcal mol^{-1} and leads to the stable formation of intermediate **E** (−64.9 kcal mol^{-1}). The latter exchanges an isonitrile with two THF molecules to yield the experimentally observed complex **9a**. This ligand exchange is very exothermic in line with the crystallization of complex **9a** (Scheme S32 in the ESI†).

Our attempts to isolate the isonitrile coordinated intermediates to prove the coordinative (or nucleophilic) ability of the nitriles in the formation of complexes **6**, **7** and **9** are not successful. Then, the non-THF coordinated complexes **3** bearing the amino-functionalized enolate chelate ligands were synthesized, and their reactivity towards isonitriles was studied. To our delight, the ^{t}OctylNC coordinated (Yb–$C_{CNtOctyl}$ bond lengths of 2.656(9) Å) complex **10a** (Scheme 15 and Fig. S99 in the ESI†) was separated in a moderate yield from the reaction of the dinuclear ytterbium complex **3c** with 2 equiv. of ^{t}OctylNC in toluene at ambient temperature. This result supports the proposed coordination of isonitrile with Lewis acidic rare-earth metal centers and provides insights into the proposed intermediate equivalents ^{Ad}**A**, ^{Dipp}**A** and **A** in the formation of complexes **6**, **7** and **9**. Complex **10a** does not further react with excess ^{t}OctylNC on either the synthetic or NMR scale, indicating ligand effects on the reactivity. However, when dinuclear complex **3a** was treated with XylNC, complex **10b** (Scheme 15, Fig. 4 and S100 in the ESI†) bearing an aza-metallacyclobutene moiety was isolated. In **10b**, the C=C double bond ($C_{2\text{-ind}}$–$C_{isonitrile}$ = 1.383(6) Å, and $C_{isonitrile}$–$N_{isonitrile}$ = 1.388(6) Å) is different from the aza-metallacyclobutene having a C=N double bond ($C_{2\text{-ind}}$–$C_{isonitrile}$ = 1.510(10) Å, $C_{isonitrile}$–$N_{isonitrile}$ = 1.385(10) Å) in the four-membered ring in complexes **6**. It is proposed that the formation of **10b** involves coordination of the isonitrile to the metal centre to give the intermediate **10a**, which then undergoes 1,1-migratory insertion to generate the ketenimine intermediate. The ketenimine inserts into the RE–$C_{CH_2\text{-}SiMe_3}$ bonds to deliver the final products, which is also different from that in the formation of **6** (Scheme S33 in the ESI†).

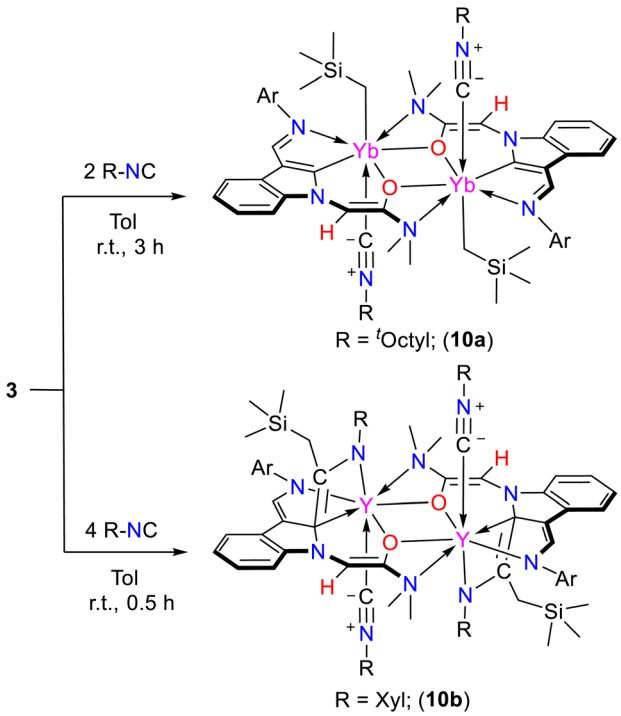

Scheme 15 The reactions of complexes **3** with isonitriles.

This reactivity pattern is different from those in the formation of complexes **6**, **7** and **9** highlighting again the influence of ligands on the reactivity patterns. Thus, four different reactivity patterns were found in the reactions of the synthesized rare-earth metal complexes with isonitriles: (1) replacement of THF of complexes **1** by isonitriles affords the isonitrile coordinated intermediates, which then undergo a stepwise 1,1-isonitrile migratory insertion to the carbene carbon to generate the intermediates having imidoyl anion attached to the indol-2-yl carbon *via* intramolecular redox. The imidoyl anion abstracts proton of the α C–H of the amidate to produce the final complexes **6** containing the aza-metallacyclobutene with a C=N

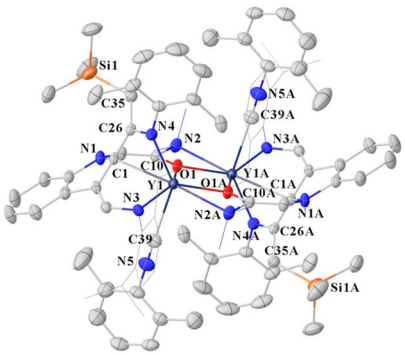

Fig. 4 Molecular structure of **10b** with the thermal ellipsoid at 30% probability level. All hydrogen atoms were omitted and the diisopropylphenyl (Dipp) group was drawn in wireframe style for clarity. Selected bond lengths (Å) and selected bond angles (deg) can be read in the ESI.†

double bond. (2) The stepwise coordination and 1,1-isonitrile migratory insertion with subsequent isomerization with complexes **2** produce the ketenimine intermediate, which then was attached by the amido nitrogen to generate [4 + 1] annulation products of the indolo-fused 2-amido-functionalized pyrrolyl ligated complexes **7**. (3) Coordination of the polarized isonitrile to the metal centre to produce a more electrophilic indol-2-yl carbon followed by 1,1-isonitrile migratory insertion to give the ketenimine intermediate. A second molecule of isonitrile undergoes a nucleophilic addition to the central carbon of the ketenimine yielding another ketenimine intermediate which is attached by the amido nitrogen followed by coordination with two molecules of THF to form the unprecedented aza-[4 + 1 + 1] annulation product **9**. (4) Coordination of the isonitrile to the metal centre followed by 1,1-isonitrile migratory insertion to give the ketenimine intermediate, which then inserts into the RE–$C_{CH_2SiMe_3}$ bond to produce the complexes **10** with aza-metallacyclobutene motifs having a C=C double bond.

Conclusions

In summary, three different types of novel rare-earth metal complexes bearing 1-multi-chelated amidate-3-imino functionalized indol-2-yl pincer ligands (complexes **1** and **2**) or 1-multi-chelated amino-functionalized enolate-3-imino functionalized indol-2-yl pincer ligand (complexes **3**) were synthesized with rationally designed ligands. DFT calculations and experimental results reveal that the indol-2-yl carbon atoms of the ligands in the complexes can be described as ambiphilic carbenes, which display unprecedented selective reactivity towards electrophiles and nucleophiles. The RE–$C_{2\text{-ind}}$ bonds (or RE–$C_{carbene}$ bonds) of these complexes exhibit unexpected selective reactivity towards electrophiles like carbodiimides or imine to generate unusual [2 + 2] cyclometallation products of the aza-metallacyclobutane moiety. The reactions of these complexes with diphenyldiazomethane Ph_2CN_2 produce either insertion complexes or a rare complex bearing an indolo-fused six-membered ring *via* [3 + 3] annulation, depending on the amount of Ph_2CN_2. The RE–$C_{carbene}$ bonds also show selective reactivity towards Lewis acidic compounds such as AlR_3 (R = Me, Et) and 9-BBN to produce alumina- or bora-four-membered metallacycles with short RE–H–C interactions. The reactions of the newly synthesized complexes and complexes bearing electrophilic carbene and metallacyclopropane with isonitriles display four types of unique selective reactivity patterns of the carbenes: (1) the replacement of coordinated THF by isonitriles followed by 1,1-isonitrile migratory insertion to the carbene carbon with subsequent intramolecular redox and abstraction of proton of the α C–H of the amidate to generate the formal [2 + 2] cyclometallation products of aza-metallacyclobutene having a C=N double bond; (2) the substitution of THF by isonitriles followed by 1,1-isonitrile migratory insertion to the carbene carbon and isomerization to the ketenimine intermediate, which was then attacked by the nitrogen of the ligands with subsequent α C–H activation by the RE–CH_2SiMe_3 to deliver the novel aza-[4 + 1] annulation products of 1-(amido-functionalized enolate)-indolo-fused-2-amido-pyrrolyl ligated complexes; (3) coordination of the polarized isonitrile to the metal centre to produce a more electrophilic indol-2-yl carbon followed by 1,1-isonitrile migratory insertion to give the ketenimine intermediate. A second molecule of isonitrile undergoes a nucleophilic addition to the central carbon of the ketenimine yielding another ketenimine intermediate which is attached by amido nitrogen followed by coordination with two molecules THF to form the unprecedented aza-[4 + 1 + 1] annulation products; (4) the coordination of the isonitrile with subsequent 1,1-isonitrile migratory insertion into the carbene carbon and isomerization to a ketenimine intermediate, which then gets inserted into the RE–$C_{CH_2SiMe_3}$ bond to generate the multi-substituted [2 + 2] cyclometallation products of aza-metallacyclobutene having a C=C double bond. This work provides plenty of insights into the reactivity of rare-earth metal complexes bearing both ambiphilic carbene and nucleophilic carbon atoms, and demonstrates unique selective reactivity patterns of the rare-earth metal ambiphilic carbenes, which may be applicable in understanding and designing new catalytic reactions. Further work in this field is in progress.

Data availability

Experimental procedures, X-ray crystallographic details, NMR spectroscopy data, and computational details are available in the ESI.† CCDC 2258652–2258653, 2386247–2386289, 2258655, 2278784, 2278786 and 2278788 contain the supplementary crystallographic data for this paper.

Author contributions

F. Chai led and performed the synthesis, reactivity study of the amido-functionalized indol-2-yl rare-earth metal complexes and experiments for the characterization of the complexes, and manuscript draft writing. W. Wu led and performed the synthesis, reactivity study of the indol-2-yl rare-earth carborynebased metallacyclopropanes and experiments for the characterization of the complexes. T. Rajeshkumar performed the DFT calculations and analyse the results under the supervision of L. Maron, Z. Huang, Q. Yuan and Y. Wei assisted in the analysis of experimental data. L. Maron supervised and participated in the discussion on DFT calculation results. S. Wang is responsible for the project design, discussion, manuscript writing, and editing.

Conflicts of interest

There are no conflicts to declare.

Acknowledgements

Financial support for this work was provided by the National Natural Science Foundation of China (No. 22031001, U23A2079 and 22301005). The authors are thankful for the grants from the Anhui Province (202305a12020018, GXXT-2021-052) and the Wuhu Science and Technology project (2023jc16). We

appreciate the help of Dongjing Hong (Anhui Normal University) in the crystal data process and structure solution and refinement.

Notes and references

1 (*a*) H. Nishiyama, *Chem. Soc. Rev.*, 2007, **36**, 1133–1141; (*b*) J. Choi, A. H. R. MacArthur, M. Brookhart and A. S. Goldman, *Chem. Rev.*, 2011, **111**, 1761–1779; (*c*) N. Selander and K. J. Szabó, *Chem. Rev.*, 2011, **111**, 2048–2076.

2 (*a*) C. Allais, J.-M. Grassot, J. Rodriguez and T. Constantieux, *Chem. Rev.*, 2014, **114**, 10829–10868; (*b*) C. Gunanathan and D. Milstein, *Chem. Rev.*, 2014, **114**, 12024–12087; (*c*) A. Kumar, T. M. Bhatti and A. S. Goldman, *Chem. Rev.*, 2017, **117**, 12357–12384; (*d*) E. Peris and R. H. Crabtree, *Chem. Soc. Rev.*, 2018, **47**, 1959–1968; (*e*) A. Haque, L. Xu, R. A. Al-Balushi, M. K. Al-Suti, R. Ilmi, Z. L. Guo, M. S. Khan, W.-Y. Wong and P. R. Raithby, *Chem. Soc. Rev.*, 2019, **48**, 5547–5563; (*f*) L. Alig, M. Fritz and S. Schneider, *Chem. Rev.*, 2019, **119**, 2681–2751; (*g*) G. Kleinhans, A. J. Karhu, H. Boddaert, S. Tanweer, D. Wunderlin and D. I. Bezuidenhout, *Chem. Rev.*, 2023, **123**, 8781–8858.

3 M. A. W. Lawrence, K.-A. Green, P. N. Nelson and S. C. Lorraine, *Polyhedron*, 2018, **143**, 11–27.

4 (*a*) Y. Pan, T. Xu, G.-W. Yang, K. Jin and X.-B. Lu, *Inorg. Chem.*, 2013, **52**, 2802–2808; (*b*) J. Zhang, H. Yao, Y. Zhang, H. Sun and Q. Shen, *Organometallics*, 2008, **27**, 2672–2675; (*c*) A. Adhikary, S. Saha, N. S. Kumar, A. G. Oliver, J. A. Krause and H. Guan, *Organometallics*, 2023, **42**, 1525–1537.

5 (*a*) V. Rad'kov, V. Dorcet, J.-F. Carpentier, A. Trifonov and E. Kirillov, *Organometallics*, 2013, **32**, 1517–1527; (*b*) D. Sengupta, R. Bhattacharjee, R. Pramanick, S. P. Rath, N. S. Chowdhury, A. Datta and S. Goswami, *Inorg. Chem.*, 2016, **55**, 9602–9610; (*c*) R. Pramanick, R. Bhattacharjee, D. Sengupta, A. Datta and S. Goswami, *Inorg. Chem.*, 2018, **57**, 6816–6824.

6 (*a*) L. Wang, D. Liu and D. Cui, *Organometallics*, 2012, **31**, 6014–6021; (*b*) P. Zhang, H. Liao, H. Wang, X. Li, F. Yang and S. Zhang, *Organometallics*, 2017, **36**, 2446–2451; (*c*) M.-C. Chang, A. J. McNeece, E. A. Hill, A. S. Filatov and J. S. Anderson, *Chem. Eur. J.*, 2018, **24**, 8001–8008.

7 (*a*) K. R. D. Johnson, B. L. Kamenz and P. G. Hayes, *Organometallics*, 2014, **33**, 3005–3011; (*b*) K. R. D. Johnson and P. G. Hayes, *Organometallics*, 2013, **32**, 4046–4049.

8 (*a*) D. V. Gutsulyak, W. E. Piers, J. Borau-Garcia and M. Parvez, *J. Am. Chem. Soc.*, 2013, **135**, 11776–11779; (*b*) E. A. LaPierre, W. E. Piers, D. M. Spasyuk and D. W. Bi, *Chem. Commun.*, 2016, **52**, 1361–1364; (*c*) W. Ren, H. Liu, F. You, P. Mao, Y.-M. So, X. Kang and X. Shi, *Dalton Trans.*, 2021, **50**, 1334–1343; (*d*) Q. Zhuo, J. Yang, X. Zhou, T. Shima, Y. Luo and Z. Hou, *J. Am. Chem. Soc*, 2023, **145**, 22803–22813; *J. Am. Chem. Soc.*, 2024, **146**, 10984–10992; (*e*) T. Shima, Q. Zhuo, X. Zhou, P. Wu, R. Owada, G. Luo and Z. Hou, *Nature*, 2024, **632**, 307–312.

9 (*a*) X.-Y. Cao, Q. Zhao, Z. Lin and H. Xia, *Acc. Chem. Res.*, 2014, **47**, 341–354; (*b*) D. Chen, Y. Hua and H. Xia, *Chem. Rev.*, 2020, **120**, 12994–13086; (*c*) Q. Li, Y. Hua, C. Tang, D. Chen, M. Luo and H. Xia, *J. Am. Chem. Soc.*, 2023, **145**, 7580–7591.

10 (*a*) S. Zhu, W. Xu, D. Hong, W. Wu, F. Chai, X. Zhu, S. Zhou and S. Wang, *Inorg. Chem.*, 2023, **62**, 381–391; (*b*) Z. Huang, S. Wang, X. Zhu, Y. Wei, Q. Yuan, S. Zhou, X. Mu and H. Wang, *Chin. J. Chem.*, 2021, **39**, 3360–3368; (*c*) Y. Wei, Q. Bao, L. Song, D. Hong, J. Gao, S. Wang, X. Zhu, S. Zhou and X. Mu, *Dalton Trans.*, 2022, **51**, 2953–2961; (*d*) Z. Zhao, Y. Tong, C. Liu, Z. Huang, S. Wang and F. Wang, *New J. Chem.*, 2024, **48**, 14690–14696.

11 (*a*) W. J. Evans, J. C. Brady and J. W. Ziller, *Inorg. Chem.*, 2002, **41**, 3340–3346; (*b*) X. Zhu, S. Wang, S. Zhou, Y. Wei, L. Zhang, F. Wang, Z. Feng, L. Guo and X. Mu, *Inorg. Chem.*, 2012, **51**, 7134–7143; (*c*) Z. Feng, X. Zhu, S. Wang, S. Zhou, Y. Wei, G. Zhang, B. Deng and X. Mu, *Inorg. Chem.*, 2013, **52**, 9549–9556; (*d*) L. Guo, X. Zhu, G. Zhang, Y. Wei, L. Ning, S. Zhou, Z. Feng, S. Wang, X. Mu, J. Chen and Y. Jiang, *Inorg. Chem.*, 2015, **54**, 5725–5731; (*e*) L. Guo, S. Wang, Y. Wei, S. Zhou, X. Zhu and X. Mu, *Inorg. Chem.*, 2017, **56**, 6197–6207; (*f*) D. Hong, X. Zhu, S. Wang, Y. Wei, S. Zhou, Z. Huang, S. Zhu, R. Wang, W. Yue and X. Mu, *Dalton Trans.*, 2019, **48**, 5230–5242; (*g*) S. Zhu, W. Wu, D. Hong, F. Chai, Z. Huang, X. Zhu, S. Zhou and S. Wang, *Inorg. Chem.*, 2024, **63**, 14860–14875.

12 S. A. Ryken and L. L. Schafer, *Acc. Chem. Res.*, 2015, **48**, 2576–2586.

13 S. Liu, W. Sun, Y. Zeng, D. Wang, W. Zhang and Y. Li, *Organometallics*, 2010, **29**, 2459–2464.

14 (*a*) L. J. E. Stanlake, J. D. Beard and L. L. Schafer, *Inorg. Chem.*, 2008, **47**, 8062–8068; (*b*) W. Zhang, Y. Wang, J. Cao, L. Wang, Y. Pan, C. Redshaw and W.-H. Sun, *Organometallics*, 2011, **30**, 6253–6261.

15 (*a*) Z. Zhang and L. L. Schafer, *Org. Lett.*, 2003, **5**, 4733–4736; (*b*) R. K. Thomson, J. A. Bexrud and L. L. Schafer, *Organometallics*, 2006, **25**, 4069–4071; (*c*) L. J. E. Stanlake and L. L. Schafer, *Organometallics*, 2009, **28**, 3990–3998; (*d*) E. Chong and L. L. Schafer, *Org. Lett.*, 2013, **15**, 6002–6005; (*e*) D. C. Leitch, R. H. Platel and L. L. Schafer, *J. Am. Chem. Soc.*, 2011, **133**, 15453–15463; (*f*) E. Chong, J. W. Brandt and L. L. Schafer, *J. Am. Chem. Soc.*, 2014, **136**, 10898–10901; (*g*) J. W. Brandt, E. Chong and L. L. Schafer, *ACS Catal.*, 2017, **7**, 6323–6330; (*h*) H. Hao and L. L. Schafer, *ACS Catal.*, 2020, **10**, 7100–7111; (*i*) H. Hao, T. Bagnol, M. Pucheault and L. L. Schafer, *Org. Lett.*, 2021, **23**, 1974–1979.

16 (*a*) P. L. Arnold and I. J. Casely, *Chem. Rev.*, 2009, **109**, 3599–3611; (*b*) J. C. Y. Lin, R. T. W. Huang, C. S. Lee, A. Bhattacharyya, W. S. Hwang and I. J. B. Lin, *Chem. Rev.*, 2009, **109**, 3561–3598; (*c*) K. H. Dötz and J. Stendel, *Chem. Rev.*, 2009, **109**, 3227–3274; (*d*) A. A. Danopoulos, T. Simler and P. Braunstein, *Chem. Rev.*, 2019, **119**, 3730–3961; (*e*) Á. Vivancos, C. Segarra and M. Albrecht, *Chem. Rev.*, 2018, **118**, 9493–9586; (*f*) K. M. Hindi, M. J. Panzner, C. A. Tessier, C. L. Cannon and W. J. Youngs, *Chem. Rev.*,

2009, **109**, 3859–3884; (*g*) H. Amouri, *Chem. Rev.*, 2023, **123**, 230–270.

17 (*a*) A. A. Danopoulos, N. Tsoureas, J. C. Green and M. B. Hursthous, *Chem. Commun.*, 2003, 756–757; (*b*) T. Steninke, B. K. Shaw, H. Jong, B. O. Patrick, M. D. Fryzuk and J. C. Green, *J. Am. Chem. Soc.*, 2009, **131**, 10461–10466; (*c*) C. Romain, K. Miqueu, J.-M. Sotiropoulos, S. Bellemin-Laponnaz and S. Dagorne, *Angew. Chem., Int. Ed.*, 2010, **49**, 2198–2201; (*d*) E. Despagnet-Ayoub, L. M. Henling, J. A. Labinger and J. E. Bercaw, *Organometallics*, 2013, **32**, 2934–2938; (*e*) T. Hatanaka, Y. Ohki and K. Tatsumi, *Angew. Chem., Int. Ed.*, 2014, **53**, 2727–2729; (*f*) E. Despagnet-Ayoub, M. K. Takase, J. A. Labinger and J. E. Bercaw, *J. Am. Chem. Soc.*, 2015, **137**, 10500–10503; (*g*) C. Romain, D. Specklin, K. Miqueu, J.-M. Sotiropoulos, C. Fliedel, S. Bellemin-Laponnaz and S. Dagorne, *Organometallics*, 2015, **34**, 4854–4863; (*h*) R. M. Brown, J. B. Garcia, J. Valjus, C. J. Roberts, H. M. Tuononen, M. Parvez and R. Roesler, *Angew. Chem., Int. Ed.*, 2015, **54**, 6274–6277; (*i*) X. Ren, C. Gourlaouen, M. Wesolek and P. Braunstein, *Angew. Chem., Int. Ed.*, 2017, **56**, 12557–12560; (*j*) C. C. Quadri, R. Lalrempuia, J. Hessevik, K. W. Törnroos and E. L. Roux, *Organometallics*, 2017, **36**, 4477–4489; (*k*) M. T. Nguyen, D. Gusev, A. Dmitrienko, B. M. Gabidullin, D. Spasyuk, M. Pilkington and G. I. Nikonov, *J. Am. Chem. Soc.*, 2020, **142**, 5852–5861; (*l*) K. Lubitz and U. Radius, *Organometallics*, 2019, **38**, 2558–2572; (*m*) F. He, C. Gourlaouen, H. Pang and P. Braunstein, *Chem. Eur. J.*, 2022, **28**, e202104234.

18 Z. Huang, R. Wang, T. Sheng, X. Zhong, S. Wang, X. Zhu, Q. Yuan, Y. Wei and S. Zhou, *Inorg. Chem.*, 2021, **60**, 18843–18853.

19 (*a*) D. Hong, T. Rajeshkumar, S. Zhu, Z. Huang, S. Zhou, X. Zhu, L. Maron and S. Wang, *Sci. China Chem.*, 2023, **66**, 117–126; (*b*) W. Wu, T. Rajeshkumar, D. Hong, S. Zhu, Z. Huang, F. Chai, W. Wang, Q. Yuan, Y. Wei, Z. Xie, L. Maron and S. Wang, *Inorg. Chem.*, 2024, **63**, 18365–18378; (*c*) W. Wu, T. Rajeshkumar, S. Zhu, F. Chai, D. Hong, Z. Huang, Q. Yuan, L. Maron and S. Wang, *Chem. Sci.*, 2024, **15**, 20315–20327.

20 (*a*) M. Scholl, S. Ding, C. W. Lee and R. H. Grubbs, *Org. Lett.*, 1999, **1**, 953–956; (*b*) S. Díez-González, N. Marion and S. P. Nolan, *Chem. Rev.*, 2009, **109**, 3612–3676; (*c*) N. I. Saper and J. F. Hartwig, *J. Am. Chem. Soc.*, 2017, **139**, 17667–17676; (*d*) H. M. O'Brien, M. Manzotti, R. D. Abrams, D. Elorriaga, H. A. Sparkes, S. A. Davis and R. B. Bedford, *Nat. Catal.*, 2018, **1**, 429–437; (*e*) Y. Tang, I. Benaissa, M. Huynh, L. Vendier, N. Lugan, S. Bastin, P. Belmont, V. César and V. Michelet, *Angew. Chem., Int. Ed.*, 2019, **58**, 7977–7981; (*f*) J. Sun, L. Luo, Y. Luo and L. Deng, *Angew. Chem., Int. Ed.*, 2017, **56**, 2720–2724; (*g*) J. Cheng, L. J. Wang, P. Wang and L. Deng, *Chem. Rev.*, 2018, **118**, 9930–9987; (*h*) M. Iglesias and L. A. Oro, *Chem. Soc. Rev.*, 2018, **47**, 2772–2808; (*i*) A. A. Danopoulos, T. Simler and P. Braunstein, *Chem. Rev.*, 2019, **119**, 3730–3961; (*j*) Q. Zhao, G. R. Meng, M. Szostak and S. P. Nolan, *Chem. Rev.*, 2020, **120**, 1981–2048; (*k*) K. Balayan, H. Sharma, K. Vsnks, S. Ravindranathan, R. G. Gonnade and S. S. Sen, *Chem. Commun.*, 2023, **59**, 8540–8543; (*l*) P. Parvathy and P. Parameswaran, *Chem. Eur. J.*, 2023, **29**, e202300582.

21 (*a*) V. Lavallo, Y. Canac, C. Präsang, B. Donnadieu and G. Bertrand, *Angew. Chem., Int. Ed.*, 2005, **44**, 5705; (*b*) M. Melaimi, R. Jazzar, M. Soleilhavoup and G. Bertrand, *Angew. Chem., Int. Ed.*, 2017, **56**, 10046–10068; (*c*) S. Termühlen, J. Blumenberg, A. Hepp, C. G. Daniliuc and F. E. Hahn, *Angew. Chem., Int. Ed.*, 2021, **60**, 2599–2602.

22 (*a*) V. Lavallo, G. D. Frey, B. Donnadieu, M. Soleilhavoup and G. Bertrand, *Angew. Chem., Int. Ed.*, 2008, **47**, 5224–5228; (*b*) V. M. Marx, A. H. Sullivan, M. Melaimi, S. C. Virgil, B. K. Keitz, D. S. Weinberger, G. Bertrand and R. H. Grubbs, *Angew. Chem., Int. Ed.*, 2015, **54**, 1919–1923; (*c*) G. Ung and J. C. Peters, *Angew. Chem., Int. Ed.*, 2015, **54**, 532–535; (*d*) Y. Wei, B. Rao, X. Cong and X. Zeng, *J. Am. Chem. Soc.*, 2015, **137**, 9250–9253; (*e*) M. P. Wiesenfeldt, Z. Nairoukh, W. Li and F. Glorius, *Science*, 2017, **357**, 908–912; (*f*) D. L. Nascimento and D. E. Fogg, *J. Am. Chem. Soc.*, 2019, **141**, 19236–19240.

23 (*a*) D. Di, A. S. Romanov, L. Yang, J. M. Richter, J. P. H. Rivett, S. Jones, T. H. Thomas, M. A. Jalebi, R. H. Friend, M. Linnolahti, M. Bochmann and D. Credgington, *Science*, 2017, **356**, 159–163; (*b*) A. S. Romanov, C. R. Becker, C. E. James, D. Di, D. Credgington, M. Linnolahti and M. Bochmann, *Chem. Eur. J.*, 2017, **23**, 4625–4637; (*c*) R. Hamze, J. L. Peltier, D. Sylvinson, M. Jung, J. Cardenas, R. Haiges, M. Soleilhavoup, R. Jazzar, P. I. Djurovich, G. Bertrand and M. E. Thompson, *Science*, 2019, **363**, 601–606; (*d*) M. Deng, N. F. M. Mukthar, N. D. Schley and G. Ung, *Angew. Chem., Int. Ed.*, 2020, **59**, 1228–1231.

24 V. Lavallo, Y. Canac, B. Donnadieu, W. W. Schoeller and G. Bertrand, *Angew. Chem., Int. Ed.*, 2006, **45**, 3488–3491.

25 J. D. Masuda, W. W. Schoeller, B. Donnadieu and G. Bertrand, *Angew. Chem., Int. Ed.*, 2007, **46**, 7052–7055.

26 (*a*) G. D. Frey, V. Lavallo, B. Donnadieu, W. W. Schoeller and G. Bertrand, *Science*, 2007, **316**, 439–441; (*b*) G. D. Frey, J. D. Masuda, B. Donnadieu and G. Bertrand, *Angew. Chem., Int. Ed.*, 2010, **49**, 9444–9447; (*c*) A. V. Zhukhovitskiy, M. G. Mavros, K. T. Queeney, T. Wu, T. V. Voorhis and J. A. Johnson, *J. Am. Chem. Soc.*, 2016, **138**, 8639–8652; (*d*) S. Würtemberger-Pietsch, H. Schneider, T. B. Marder and U. Radius, *Chem. Eur. J.*, 2016, **22**, 13032–13036; (*e*) A. Bakker, M. Freitag, E. Kolodzeiski, P. Bellotti, A. Timmer, J. Ren, B. S. Lammers, D. Moock, H. W. Roesky, H. Mönig, S. Amirjalayer, H. Fuchs and F. Glorius, *Angew. Chem. Int. Ed.*, 2020, **59**, 13643–13646; (*f*) G. Kaur, R. L. Thimes, J. P. Camden and D. M. Jenkins, *Chem. Commun.*, 2022, **58**, 13188–13197; (*g*) A. V. Zhukhovitskiy, M. G. Mavros, K. T. Queeney, T. Wu, T. V. Voorhis and J. A. Johnson, *J. Am. Chem. Soc.*, 2016, **138**, 8639–8652; (*h*) C. A. Smith, M. R. Narouz, P. A. Lummis, I. Singh, A. Nazemi, C.-H. Li and C. M. Crudden, *Chem. Rev.*, 2019, **119**, 4986–5056.

27 (*a*) T. W. Hudnall and C. W. Bielawski, *J. Am. Chem. Soc.*, 2009, **131**, 16039–16041; (*b*) M. Braun, W. Frank, G. J. Reiss and C. Ganter, *Organometallics*, 2010, **29**, 4418–4420; (*c*) Z. R. McCarty, D. N. Lastovickova and C. W. Bielawski, *Chem. Commun.*, 2016, **52**, 5447–5450; (*d*) M. B. Gildner and T. W. Hudnall, *Chem. Commun.*, 2019, **55**, 12300–12303; (*e*) P. R. Sultane, G. Ahumada, D. Janssen-Müller and C. W. Bielawski, *Angew. Chem. Int. Ed.*, 2019, **58**, 16320–16325; (*f*) M. Košutić, S. Neuner, A. Ren, S. Flür, C. Wunderlich, E. Mairhofer, N. Vušurović, J. Seikowski, K. Breuker, C. Höbartner, D. J. Patel, C. Kreutz and R. Micura, *Angew. Chem. Int. Ed.*, 2015, **54**, 15128–15133; (*g*) H. Song, H. Kim and E. Lee, *Angew. Chem. Int. Ed.*, 2018, **57**, 8603–8607; (*h*) D. Martin, N. Lassauque, B. Donnadieu and G. Bertrand, *Angew. Chem., Int. Ed.*, 2012, **51**, 6172–6175; (*i*) M. J. López-Gómez, D. Martin and G. Bertrand, *Chem. Commun.*, 2013, **49**, 4483–4485; (*j*) E. Tomás-Mendivil, M. M. Hansmann, C. M. Weinstein, R. Jazzar, M. Melaimi and G. Bertrand, *J. Am. Chem. Soc.*, 2017, **139**, 7753–7756; (*k*) C. M. Weinstein, G. P. Junor, D. R. Tolentino, R. Jazzar, M. Melaimi and G. Bertrand, *J. Am. Chem. Soc.*, 2018, **140**, 9255–9260; (*l*) Z. R. Turner, *Chem. Eur. J.*, 2016, **22**, 11461–11468.

28 (*a*) A. Dömling, *Chem. Rev.*, 2006, **106**, 17–89; (*b*) C. D. Graaff, E. Ruijter and R. V. A. Orru, *Chem. Soc. Rev.*, 2012, **41**, 3969–4009; (*c*) A. Dömling, W. Wang and K. Wang, *Chem. Rev.*, 2012, **112**, 3083–3135.

29 (*a*) J. Fernández-Gallardo, L. Bellarosa, G. Ujaque, A. Lledós, M. J. Ruiz, R. Fandos and A. Otero, *Organometallics*, 2012, **31**, 7052–7062; (*b*) Y. Zhang, R. J. Keaton and L. R. Sita, *J. Am. Chem. Soc.*, 2003, **125**, 8746–8747; (*c*) E. Barnea, T. Andrea, J.-C. Berthet, M. Ephritikhine and M. S. Eisen, *Organometallics*, 2008, **27**, 3103–3112; (*d*) L. Pauly, A. K. Adegboyega, C. A. Brown, D. E. Pérez and E. A. Ison, *Organometallics*, 2024, **43**, 3002–3012.

30 (*a*) E. Lu, Y. Chen and X. Leng, *Organometallics*, 2011, **30**, 5433–5441; (*b*) J. Zhang, W. Yi, Z. Zhang, Z. Chen and X. Zhou, *Organometallics*, 2011, **30**, 4320–4324; (*c*) G. P. McGovern, F. Hung-Low, J. W. Tye and C. A. Bradley, *Organometallics*, 2012, **31**, 3865–3879; (*d*) C. S. Weinert, P. E. Fanwick and I. P. Rothwell, *Organometallics*, 2005, **24**, 5759–5766; (*e*) R. Fandos, J. Fernández-Gallardo, A. Otero, A. Rodríguez and M. J. Ruiz, *Organometallics*, 2011, **30**, 1551–1557; (*f*) J. Fernández-Gallardo, A. Bajo, R. Fandos, A. Otero, A. Rodrıguez and M. J. Ruiz, *Organometallics*, 2013, **32**, 1752–1758.

31 (*a*) S. N. MacMillan, J. M. Tanski and R. Waterman, *Chem. Commun.*, 2007, 4172–4174; (*b*) A. J. Roering, J. J. Davidson, S. N. MacMillan, J. M. Tanski and R. Waterman, *Dalton Trans.*, 2008, 4488–4498; (*c*) A. F. Maddox, J. J. Davidson, T. Shalumova, J. M. Tanski and R. Waterman, *Inorg. Chem.*, 2013, **52**, 7811–7816; (*d*) S. Clément, L. Guyard, M. Knorr, S. Dilsky, C. Strohmann and M. Arroyo, *J. Organomet. Chem.*, 2007, **692**, 839–850; (*e*) S. Clément, S. M. Aly, D. Bellows, D. Fortin, C. Strohmann, L. Guyard, A. S. Abd-El-Aziz, M. Knorr and P. D. Harvey, *Inorg. Chem.*, 2009, **48**, 4118–4133.

32 (*a*) M. D. Fryzuk, P. B. Duval, S. S. S. H. Mao, S. J. Rettig, M. J. Zaworotko and L. R. MacGillivray, *J. Am. Chem. Soc.*, 1999, **121**, 1707–1716; (*b*) F. Basuli, B. C. Bailey, L. A. Watson, J. Tomaszewski, J. C. Huffman and D. J. Mindiola, *Organometallics*, 2005, **24**, 1886–1906; (*c*) D. J. Yarrow, J. A. Ibers, Y. Tatsuno and S. Otsuka, *J. Am. Chem. Soc.*, 1973, **95**, 8590–8597; (*d*) T. Sielisch and U. Behrens, *J. Organomet. Chem.*, 1986, **310**, 179–187; (*e*) R. Aumann and H. Heinen, *Chem. Ber.*, 1988, **121**, 1085–1091; (*f*) I. Fernández, F. P. Cossío and M. A. Sierra, *Organometallics*, 2007, **26**, 3010–3017; (*g*) K. G. Moloy, P. J. Fagan, J. M. Manriquez and T. J. Marks, *J. Am. Chem. Soc.*, 1986, **108**, 56–67; (*h*) F. Basuli, B. C. Bailey, D. Brown, J. Tomaszewski, J. C. Huffman, M. H. Baik and D. J. Mindiola, *J. Am. Chem. Soc.*, 2004, **126**, 10506–10507; (*i*) J. B. Russell, M. G. Jafari, J. H. Kim, B. Pudasaini, A. Ozarowski, J. Telser, M. H. Baik and D. J. Mindiola, *Angew. Chem., Int. Ed.*, 2024, **63**, e202401433.

33 B. F. Wicker, M. Pink and D. J. Mindiola, *Dalton Trans.*, 2011, **40**, 9020–9025.

34 (*a*) P. S. Pregosin, *NMR in Organometallic Chemistry*, Wiley-VCH, Weinheim, 2012; (*b*) R. B. Jordan, *Inorg. Chem.*, 2023, **62**, 3715–3721; (*c*) Z. Huang, S. Wang, X. Zhu, Q. Yuan, Y. Wei, S. Zhou and X. Mu, *Inorg. Chem.*, 2018, **57**, 15069–15078.

35 Z.-J. Lv, Z. Chai, M. Zhu, J. Wei and W. Zhang, *J. Am. Chem. Soc.*, 2021, **143**, 9151–9161.

36 J. S. Gopinath and P. Parameswaran, *Organometallics*, 2024, **43**, 1411–1424.

37 (*a*) S. Li, J. Cheng, Y. Chen, M. Nishiura and Z. Hou, *Angew. Chem., Int. Ed.*, 2011, **50**, 6360–6363; (*b*) W. Yi, J. Zhang, F. Zhang, Y. Zhang, Z. Chen and X. Zhou, *Chem. Eur. J.*, 2013, **19**, 11975–11983; (*c*) Y. Cao, Z. Du, W. Li, J. Li, Y. Zhang, F. Xu and Q. Shen, *Inorg. Chem.*, 2011, **50**, 3729–3737; (*d*) K. C. Casey, J. K. Appiah and J. R. Robinson, *Inorg. Chem.*, 2020, **59**, 14827–14837.

38 G. Zhang, S. Wang, X. Zhu, S. Zhou, Y. Wei, Z. Huang and X. Mu, *Organometallics*, 2017, **36**, 3812–3822.

39 (*a*) G. Zhang, S. Wang, S. Zhou, Y. Wei, L. Guo, X. Zhu, L. Zhang, X. Gu and X. Mu, *Organometallics*, 2015, **34**, 4251–4261; (*b*) X. Zhu, Y. Li, Y. Wei, S. Wang, S. Zhou and L. Zhang, *Organometallics*, 2016, **35**, 1838–1846; (*c*) G. Zhang, B. Deng, S. Wang, Y. Wei, S. Zhou, X. Zhu, Z. Huang and X. Mu, *Dalton Trans.*, 2016, **45**, 15445–15456; (*d*) L. Guo, X. Zhu, G. Zhang, Y. Wei, L. Ning, S. Zhou, Z. Feng, S. Wang, X. Mu, J. Chen and Y. Jiang, *Inorg. Chem.*, 2015, **54**, 5725–5731; (*e*) G. Zhang, S. Wang, X. Zhu, S. Zhou, Y. Wei, Z. Huang and X. Mu, *Organometallics*, 2017, **36**, 3812–3822; (*f*) X. Zhu, Y. Jiang, J. Chen, S. Wang, Z. Huang, S. Zhu, X. Zhao, W. Yue, J. Zhang, W. Wu and X. Zhong, *Chin. J. Chem.*, 2020, **38**, 478–488; (*g*) D. Diether, M. Meermann-Zimmermann, K. W. Törnroos, C. Maichle-Mössmer and R. Anwander, *Dalton Trans.*, 2020, **49**, 2004–2013; (*h*) M. M. Katzenmayer, B. M. Wolf, A. Mortis, C. Maichle-Mössmer and R. Anwander, *Chem. Commun.*, 2021, **57**, 243–246; (*i*) E. C. Moinet, B. M. Wolf, O. Tardif,

C. Maichle-Mössmer and R. Anwander, *Angew. Chem., Int. Ed.*, 2023, **62**, e202219316.
40 H. Nakamura, Y. Nakayama, H. Yasuda, T. Maruo, N. Kanehisa and Y. Kai, *Organometallics*, 2000, **19**, 5392–5399.
41 W. Jiang, F. Kong, I. D. Rosal, M. Li, K. Wang, L. Maron and L. Zhang, *Chem. Sci.*, 2023, **14**, 9154–9160.
42 W. Jiang, T. Rajeshkumar, M. Guo, L. Maron and L. Zhang, *Chem. Sci.*, 2024, **15**, 3495–3501.
43 M. G. Schrems, H. M. Dietrich, K. W. Tornroos and R. Anwander, *Chem. Commun.*, 2005, 5922–5924.
44 M. Zimmermann, K. W. Törnroos and R. Anwander, *Angew. Chem., Int. Ed.*, 2008, **47**, 775–778.
45 J. Klosin, G. R. Roof and E. Y. Chen, *Organometallics*, 2000, **19**, 4684–4686.
46 J. Chu, C. Wang, L. Xiang, X. Leng and Y. Chen, *Organometallics*, 2017, **36**, 4620–4625.
47 (*a*) R. D. Dicken, A. Motta and T. J. Marks, *ACS Catal.*, 2021, **11**, 2715–2734; (*b*) M. A. Iqbal, X. Yan, R. Li, F. Zhijia, S. Zhang and X. Li, *New J. Chem.*, 2024, **48**, 3149–3155.
48 (*a*) X. Chen, S. Lim, C. E. Plečnik, S. Liu, B. Du, E. A. Meyers and S. G. Shore, *Inorg. Chem.*, 2004, **43**, 692–698; (*b*) D. A. Laske, R. Duchateau, J. H. Teuben and A. L. Spek, *J. Organomet. Chem.*, 1993, **462**, 149–153; (*c*) W. J. Evans, S. E. Lorenz and J. W. Ziller, *Chem. Commun.*, 2007, 4662–4664.
49 D. Magis, J. J. Cabrera-Trujillo, J. Vignolle, J.-M. Sotiropoulos, D. Taton, K. Miqueu and Y. Landais, *J. Am. Chem. Soc.*, 2024, **146**, 16802–16813.
50 J. W. Collet, T. R. Roose, E. Ruijter, B. U. W. Maes and R. V. A. Orru, *Angew. Chem., Int. Ed.*, 2020, **59**, 540–558.
51 (*a*) W. J. Evans, J. H. Meadows, W. E. Hunter and J. L. Atwood, *Organometallics*, 1983, **2**, 1252–1254; (*b*) J. Chen, T. Chen, J. R. Norton and M. Rauch, *Organometallics*, 2018, **37**, 4424–4430.
52 D. Guo, D. Hong, Z. Huang, S. Zhou, X. Zhu and S. Wang, *Inorg. Chem.*, 2024, **63**, 9539–9551.
53 (*a*) C. Wang, W. Mao, L. Xiang, Y. Yang, J. Fang, L. Maron, X. Leng and Y. Chen, *Chem. Eur. J.*, 2018, **24**, 13903–13917; (*b*) J. Zhang, W. Yi, Z. Zhang, Z. Chen and X. Zhou, *Organometallics*, 2011, **30**, 4320–4324; (*c*) E. Lu, Y. Chen and X. Leng, *Organometallics*, 2011, **30**, 5433–5441; (*d*) N. Obata, H. Mizuno, T. Koitabashi and T. Takizawa, *B. Chem. Soc. Jpn.*, 1975, **48**, 2287–2293; (*e*) M. Pérez-Gómez, S. Hernández-Ponte, J. A. García-López, R. Frutos-Pedreño, D. Bautista, I. Saura-Llamas and J. Vicente, *Organometallics*, 2018, **37**, 4648–4663; (*f*) A. Obanda, K. Valerius, J. T. Mague, S. Sproules and J. P. Donahue, *Organometallics*, 2020, **39**, 2854–2870; (*g*) Z. Chai, J. Wei and W. Zhang, *Organometallics*, 2023, **42**, 2736–2741; (*h*) Y. Lv, C. E. Kefalidis, J. Zhou, L. Maron, X. Leng and Y. Chen, *J. Am. Chem. Soc.*, 2013, **135**, 14784–14796; (*i*) J. Chen, N. Yassin, T. Gunasekara, J. R. Norton and M. Rauch, *J. Am. Chem. Soc.*, 2018, **140**, 8980–8989; (*j*) Q. Zhuo, J. Yang, X. Zhou, T. Shima, Y. Luo and Z. Hou, *J. Am. Chem. Soc.*, 2024, **146**, 10984–10992; (*k*) C. Saviozzi, L. Biancalana, T. Funaioli, M. Bortoluzzi, M. D. Franco, M. Guelfi, V. Gandin and F. Marchetti, *Inorg. Chem.*, 2024, **63**, 1054–1067.